

Aerial Mobile Manipulation

2013 RSS Workshop on Aerial Mobile Manipulation

Organizers: Richard Voyles, Vijay Kumar and Mike Bazakos

Robotics: Science and Systems, Berlin, Germany
June 27th, Morning



The Osprey, a magnificent bird of prey that dives from undetectable heights to snatch fish from the water with its agile talons, is a master of aerial mobile manipulation. But the "snatch-and-go" is not representative of dexterous manipulation. The octopus, on the other hand, is one of the few known animals that manipulates while locomoting and does so while "flying" with great agility. Aerial mobile manipulation is a growing area of robotics research that endeavors to become the "octopus of the air" while starting out as an osprey. Capitalizing on the ubiquity of low cost and easy to fly UAVs, great strides have been made in a short time. A natural extension of the rebirth of interest in manipulation represented by the mobile manipulation community, aerial mobile manipulation addresses new challenges and overcomes new constraints not familiar to UGVs. But aerial mobile manipulation is still manipulation at heart, and manipulation requires careful attention to dynamics and collaboration which are sometimes overlooked in the practical process of defying gravity and mastering the snatch-and-go. This workshop proposes to bridge the theoretical and experimental by bringing together manipulation experts, UAV experts, real-time perception experts, and collaboration experts to present and discuss the current and future of aerial mobile manipulation.

Sponsors:

Lockheed Martin

We have an exciting program lined up!

Speakers and Topics include:

- 9:00 Welcome and Introduction of Participants
- 9:10 Oliver Brock – TU Berlin, Germany – Mobile Manipulation Overview
- 9:30 Vijay Kumar – U of Pennsylvania, USA – Aerial Mobile Manipulation Overview
- 9:40 Koushil Sreenath – U of Pennsylvania, USA – Cooperative UAV Manipulation
- 9:55 Stefano Stramigioli – U of Twente, Netherlands – About Multi-vehicle Flying Grasping
- 10:10 Mark Cutkosky – Stanford U, USA – Dynamic Surface Grasping for UAVs
- 10:25 1st Half Wrap-Up
- 10:30 coffee break and posters
- 11:00 Christos Papachristos & Anthony Tzes – U of Patras, Greece – UAVs Overcoming Physical Limitations: The Tri-TiltRotor in Obstacle Manipulation
- 11:15 Oussama Khatib – Stanford U, USA –
- 11:30 Anibal Ollero – U de Sevilla, Spain – Modeling and Control for Aerial Manipulation and Assembly in the ARCAS System
- 11:45 Rafik Mebarki, Vincenzo Lippiello & Bruno Siciliano – U di Napoli, Italy – Exploiting image moments for aerial manipulation control
- 12:00 Richard Voyles – U of Denver, USA – Dexterous Hexrotor Platform for Precision Grasping
- 12:15 Scott Morton, Vassilios Morellas & Nikos Papanikopoulos – U of Minnesota, USA – Solar-Powered Flight for Aerial Robotics
- 12:30 Lunch with discussion for research roadmap

Workshop Site

The workshop will be held in the MAR Building on the TU Berlin campus. Please refer to the [local information page](#) for a map.

Important Dates

May 8, 2013	Poster Submission Deadline
May 17, 2013	Notification of Acceptance
June 27, 9:00 am	Workshop Begins

rvoyles [at] du [dot] edu

Aerial Mobile Manipulation

Avian-Inspired Grasping for Quadrotor MAVs

Justin Thomas, Joe Polin, Giuseppe Loianno, Koushil Sreenath, and Vijay Kumar

Abstract—Micro Aerial Vehicles (MAVs) have been used in a wide range of applications [9, 7]. However, there are few papers addressing high-speed grasping and transportation of payloads using MAVs. We are interested in dynamic acquisition of targets using MAVs. Drawing inspiration from aerial hunting by birds of prey, we designed and equipped a quadrotor MAV with an actuated appendage which enabled grasping and object retrieval at high speeds. We developed a nonlinear dynamic model of the system, demonstrated that the system is differentially flat, planned dynamic trajectories using the flatness property, and presented experimental results with pick-up velocities at 2 m/s (6 body lengths / second) and 3 m/s (9 body lengths / second).

I. INTRODUCTION

Predatory birds have the ability to swiftly swoop down from great heights and grasp prey from the ground, water, and air while flying at high speeds. Although recent years have seen improvement in the capabilities of Micro Aerial Vehicles (MAVs) [6], such dynamic aerial manipulation, common in nature, has not been achieved using MAVs.

Video analysis of birds of prey, such as the bald eagle (*Haliaeetus leucocephalus*) shown in Fig. 2, reveal that an eagle sweeps its legs and claws backwards during its capture phase, thereby reducing the relative velocity between the claws of the predator and the prey [3]. This allows the bird, without slowing down, to have a near-zero relative velocity of the claw while grasping the prey.

II. DESIGN OF AN ARTICULATED GRIPPER

We use an underactuated three-fingered gripper design which allows the claw to conform to the target while being driven by a single servo motor.

To reduce the relative speed between the gripper and the target, we use the strategy employed by the eagle, which sweeps its legs backward during grasping. In particular, the gripper is mounted on a rotating arm, which is actuated by a servo motor. When the arm rotates, the gripper swings backwards which reduces the relative velocity between itself and the payload during acquisition.

III. DYNAMIC MODEL

We define x_q and z_q as the x and z positions of the quadrotor, β as the angle of the gripper arm with respect to the horizontal, and θ as the pitch of the quadrotor. The control inputs are the total thrust (u_1), the moment resulting from differential thrust (u_3), and the torque from the servo at the “hip” (τ). Then, the dynamics of the robot can be modeled

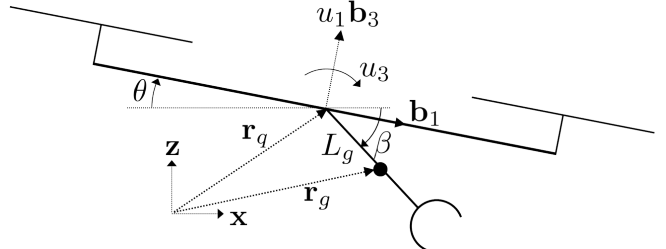


Fig. 1. The quadrotor has control inputs u_1 in the b_3 direction and u_3 as a moment about the axis into the page (b_2). The gripper forms the angle β with the horizontal and its center of mass is located a distance L_g away from the quadrotor’s center of mass.

using an Euler-Lagrange approach,

$$\dot{\mathbf{q}} = \begin{bmatrix} x_q \\ z_q \\ \theta \\ \beta \end{bmatrix}, \text{ and } \mathbf{F} = \begin{bmatrix} u_1 \sin(\theta) \\ u_1 \cos(\theta) \\ u_3 - \tau \\ \tau \end{bmatrix}$$

so that

$$\ddot{\mathbf{q}} = D^{-1} (\mathbf{F} - C\dot{\mathbf{q}} - G) \quad (1)$$

where the matrices D , C , and G are all non-zero. Note that, because of the gripper, $C \neq 0$.

IV. DIFFERENTIAL FLATNESS

The coupled system comprising of the quadrotor and the actuated gripper, whose dynamics is given by (1), is differentially flat with a set of flat outputs given by

$$\mathbf{y} = [x_q \ z_q \ \beta]^T, \quad (2)$$

Consequently, any sufficiently smooth trajectory in the flat output space is guaranteed to be dynamically feasible for the coupled system. Further, nondimensionalized kinematic analysis of an eagles motion provides boundary conditions for the motion planner.

V. RESULTS

We demonstrate experimental results on an Asctec Hummingbird quadrotor [1] equipped with a gripper. The experiments utilize the GRASP Multiple Micro UAV Testbed [8] and leverage a motion capture system to estimate the state of the quadrotor [2]. The target is a small cylinder and is tracked using VICON [2].

With this setup, the quadrotor grasped the target while moving at 2 m/s with a success rate of 100% out of 5 attempts. Additionally, the quadrotor was able to successfully grasp the target while moving at speeds up to 3 m/s, or 9 body lengths / second (Fig. 2). For more details, including a video of the experiments, see [10].



Fig. 2. A still image comparison between the eagle (extracted from [3]) and the quadrotor for a trajectory with the quadrotor moving at 3 m/s (9 body lengths / second) at pickup. See [10] for a video of the grasping.

VI. CURRENT RESEARCH

To enable dynamic grasping and perching outdoors, our current research is directed towards developing a visual servoing [4, 5] based control system, which will allow detection of a cylinder that could be used for grasping or for perching on objects such as tree branches or railings.

A diffeomorphism exists between certain image features and trajectories in the flat space. Leveraging this, we can develop a dynamic model and plan dynamically feasible trajectories in the image feature space. In addition, an image-based controller with feedback directly from the image features has been developed. Our system uses a global shutter camera with contour detection of the cylinder running at 60 Hz on a Gumstix. The approach has been verified in simple hover experiments. Finally, combining the controller with the trajectory generation, we will be able to use a single camera in the feedback loop to follow trajectories while tracking or grasping cylindrical objects.

VII. CONCLUSION

We have explored the challenges of high-speed aerial grasping using a quadrotor MAV equipped with a gripper. A novel appendage design, inspired by the articulation of an eagle's legs and claws, was shown to enable a high rate of success while grasping objects at high velocities. The dynamic model of the quadrotor and gripper system is differentially flat, and minimum snap trajectories were generated for dynamic grasping. Experimental results have been presented for quadrotor velocities of 2 m/s and 3 m/s (6 - 9 body lengths / second).

Current research focuses on the formulation of the presented strategy as a visual servoing problem, which will enable truly autonomous grasping and perching. Towards this, we have developed a vision-based controller and have shown that dynamically feasible trajectories can be planned for the image feature space. Finally, extension to the 3D case by exploiting image moments for estimation of the cylinder's orientation in the image is currently under development.

REFERENCES

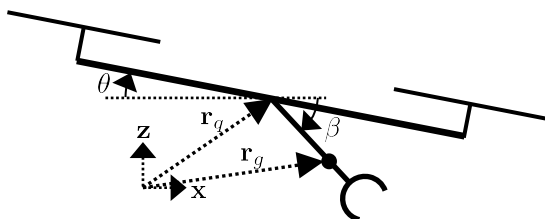
- [1] "Ascending Technologies, GmbH," <http://www.asctec.de>. URL <http://www.asctec.de/>.
- [2] "Vicon Motion Systems, Inc". URL www.vicon.com.
- [3] Karen Bass, Brian Leith, Justin Anderson, Peter Bassett, Joe Stevens, Hugh Pearson, and Jeff Turner. *Nature's Most Amazing Events*. [DVD]. BBC Worldwide Ltd. Programs, 2009.
- [4] F. Chaumette and S. Hutchinson. Visual servo control, part i: Basic approaches. *IEEE Robotics and Automation Magazine*, 13(4):82–90, December 2006.
- [5] F. Chaumette and S. Hutchinson. Visual servo control, part ii: Advanced approaches. *IEEE Robotics and Automation Magazine*, 14(1):109–118, March 2007.
- [6] Vijay Kumar and Nathan Michael. Opportunities and challenges with autonomous micro aerial vehicles. *The International Journal of Robotics Research*, 31(11):1279–1291, August 2012. ISSN 0278-3649. doi: 10.1177/0278364912455954.
- [7] Daniel Mellinger, Michael Shomin, Nathan Michael, and Vijay Kumar. Cooperative grasping and transport using multiple quadrotors. In *International Symposium on Distributed Autonomous Robotic Systems*, 2010. URL <http://www.seas.upenn.edu/~dmel/mellingerDARS10.pdf>.
- [8] Nathan Michael, Daniel Mellinger, Quentin Lindsey, and Vijay Kumar. The GRASP multiple micro-UAV testbed. *Robotics & Automation Magazine, IEEE*, 17(3):56–65, 2010.
- [9] Koushil Sreenath, Nathan Michael, and Vijay Kumar. Trajectory Generation and Control of a Quadrotor with a Cable-Suspended Load A Differentially-Flat Hybrid System. In *International Conference on Robotics and Automation*, 2013. URL <http://www.seas.upenn.edu/~koushils/ICRA2013.html>.
- [10] Justin Thomas, Joe Polin, Koushil Sreenath, and Vijay Kumar. Avian-Inspired Grasping for Quadrotor Micro UAVs. In *IDETC/CIE*, Portland, to appear 2013. URL <http://www.jtwebs.net/idetc-2013/>.

Avian-Inspired Grasping for Quadrotor MAVs

Justin Thomas, Joe Polin, Giuseppe Loianno, Koushil Sreenath, Vijay Kumar
 GRASP Lab, University of Pennsylvania

Motivation

- Prior research in aerial grasping only permitted slow, quasi-static motions.
- We are interested in rapid acquisition of targets.
- Dynamic coupling between flight, grasping, and manipulation cannot be ignored.



$$\mathbf{q} = \begin{bmatrix} x_q \\ z_q \\ \theta \\ \beta \end{bmatrix}$$

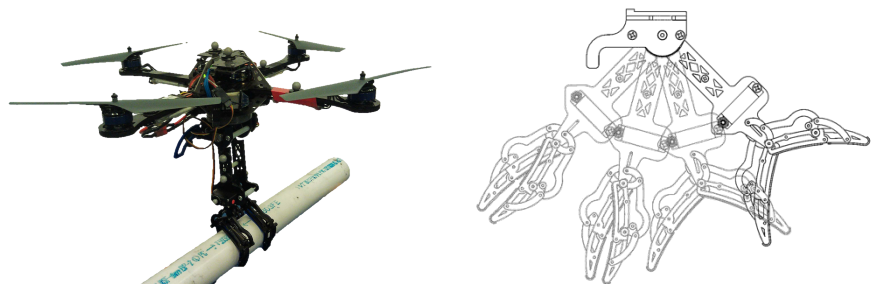
Results

- We demonstrated successful acquisition of a target while moving at 2 and 3 m/s with feedback from a motion capture system.



Gripper Design

- An underactuated gripper is attached to an articulated arm to reduce the relative velocity between the gripper and the target.
- The gripper is manufactured using laser-cut ABS.



Conclusion and Future Work

- Formulate grasping as a visual-servoing problem
- Develop image-based control algorithms with feedback from image features
- Perform onboard blob detection using a Gumstix at 60 Hz
- Extend dynamic model and differential flatness to the 3-D case
- Extend the visual-servoing to the 3-D case by considering image moments for orientation estimation of the cylinder in the image

About Multi-vehicle Flying Grasping

Stefano Stramigioli
University of Twente
The Netherlands

June 12, 2013

Abstract

In (hand) tips- grasping, an object is constrained by multiple tips of fingers which apply forces to an object. The IPC grasping controller introduced in [2], gives a physically based methodology to implement an Intrinsically Passive Control (IPC) strategy in order to grasp with either a multi finger hand or manipulation with multiple arms. This strategy has been successfully implemented and extended in different applications as also reported in [4]. The idea which is schematically reported in Fig. 1, is based on a (virtual) physically inspired controller composed of a number of geometric springs (contact springs) connecting the tips of the fingers of the hand (or the end of the multi limb system) to a virtual object. This virtual object is by itself connected to a new spring which can be used to move the all ensemble around. The goal of the virtual object is to create damping injection in the system in order to achieve a proper behaviour. The grasping is obtained by changing the lengths of the contact springs once the tips are positioned around the objects to be grasped. Changing the lengths of the springs in a geometrical consistent way, can be done as explained in [3].

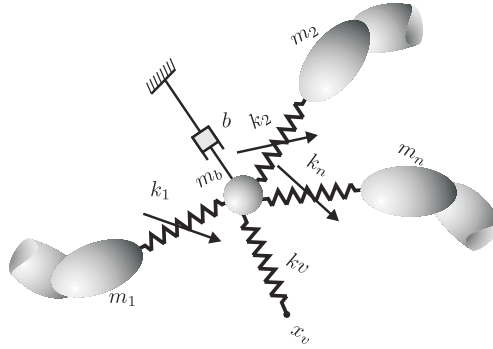


Figure 1: The main idea of the IPC grasping strategy

Porting this paradigm to a situation in which the tips are actually flying vehicles (with or without a robotic arm), adds a number of challenges to the strategy:

Distributed Architecture Each of the vehicle will have a separate processing unit and even if a central unit will be available, communication delays could destroy the passive behaviour of the physical analogy

Under-actuation The vehicles are under actuated and therefore cannot be constrained in certain direction as it is the case for a situation in which the fingers (or arms) are connected to a fixed base.

Aerodynamics Instability Contact of a flying vehicle with the environment needs special care to prevent unstable behaviour [1].

Localisation of vehicles In a manipulation with links, the joint positions of the linkages can be used to know the position of the tip which is necessary in order to implement the control law. In a flying situation this is not trivial. In an indoor situation an optical tracking system can be used, and in outdoor situations an adaptation of the algorithm should be done by relying on relative motion configurations.

In this work the first two issues of *Distributed Architecture* and *Under-Actuation* will be addressed.

References

- [1] M. Fumagalli, R. Naldi, A. Macchelli, Raffaella Carloni, Stefano Stramigioli, and L. Marconi. Modeling and control of a flying robot for contact inspection. In *Intelligent Robots and Systems (IROS), 2012 IEEE/RSJ International Conference on*, pages 3532–3537, 2012.
- [2] Stefano Stramigioli. A novel impedance grasping strategy as a generalized hamiltonian system. In D Aeyels, F. Lamnabhi-Lagarrigue, and Arjan van der Schaft, editors, *Stability and Stabilization of Nonlinear Systems, (Lecture Notes in Control and Information Sciences 246)*, volume 246 of *Lecture Notes in control and Information Sciences*, pages 293–324. Springer, London, London, 1999.
- [3] Stefano Stramigioli and Vincent Duindam. Variable Spatial Springs for Robot Control Applications. In *IROS2001: 2001 IEEE/RSJ International Conference on Intelligent Robots and Systems*, pages 1906–1911, Maui, Hawaii, October 2001. IEEE Robotics and Automation Society.
- [4] T. Wimbock, Christian Ott, Alin Albu-Schaffer, and Gerd Hirzinger. Comparison of object-level grasp controllers for dynamic dexterous manipulation. *The International Journal of Robotics Research*, 31(1):3–23, September 2011.

Dynamic Surface Grasping for UAVs

E.W. Hawkes¹, E.V. Eason², H. Jiang¹, M.A. Estrada¹, M.T. Pope¹, D.L. Christensen¹
 M.R. Cutkosky¹, A. Kehlenbeck³, J.S. Humbert³

Abstract—By employing directional adhesion, small UAVs can attach to walls and ceilings with a dynamic maneuver that absorbs kinetic energy on contact and uses it to load adhesive pads in opposition. To detach, it suffices to release the stored energy. Models of the landing process reveal design choices that satisfy constraints on the normal and tangential contact forces, so that the adhesives are loaded smoothly and without failures that could damage the mechanism or lead to slipping or bouncing off the surface. Ongoing work focuses on integrating the modeling and design of mechanisms with sensing and control during the final moments of flight to increase the robustness of the maneuver and allow for failure recovery.

I. INTRODUCTION

The ability of small UAVs to land on walls and ceilings promises to greatly expand their capabilities for applications ranging from monitoring air quality and inspecting large structures to search and rescue. While landed, they consume little power, greatly extending mission life, and provide a stable platform for sensing, communication, etc. The work described here builds upon prior work on climbing robots and the control of small rotorcraft to enable UAVs to land and perch on walls and ceilings. For rough surfaces such as concrete and brick, the grippers employ arrays of microspines inspired by the legs of insects [1]. For smooth surfaces such as glass and metal panels, they employ gecko-inspired dry adhesives [2].

The advantages of perching on surfaces have been noted, with recent developments including UAVs that grip surfaces with velcro or small grippers [3], spines [4], [1] or microstructured polymers that are peeled to detach [5].

The solutions used in the present work rely on directional adhesion. The devices are not sticky in the default state, and therefore tend not to attract dirt. With the application of a controlled tangential force, they can sustain negative normal forces. To land on ceilings and inverted surfaces it is necessary to use opposed sets of adhesives, with an internal force, f_t , applied parallel to the surface (figure 1). Relaxing this force releases the UAV. With attention to the timing of applying and relaxing internal forces, attachment and detachment can be very smooth and low-effort, resulting in long lifetimes with tens of thousands of cycles possible without large reductions in performance [6].

The sequence for landing on a surface, from first contact to equilibrium, takes less than 50 ms (figure 2). The dynamics are dominated by contact forces and there is little opportunity for aerodynamic control. This realization leads to the design

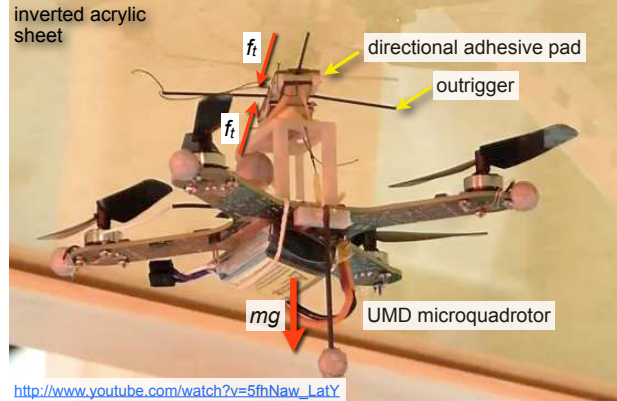


Fig. 1. An internal tangential force f_t maintains adhesion at two opposed pads, from which a 95 g UAV hangs after landing.

of a passive mechanism that can absorb the kinetic energy, using some of it to load the adhesives for attachment, and dissipating or storing the remainder.

When considering the design of the landing and attachment mechanism, it is helpful to start with functional constraints imposed by the adhesives. As seen in figure 3, for pads of directional dry adhesives, the normal and tangential forces must remain within a composite limit surface to sustain attachment. Note that increasing the magnitude of the internal force, $f_t = f_l \cos\theta$, increases the maximum downward normal force, $f_n = 2(f_l \sin\theta - f_k)$ that can be

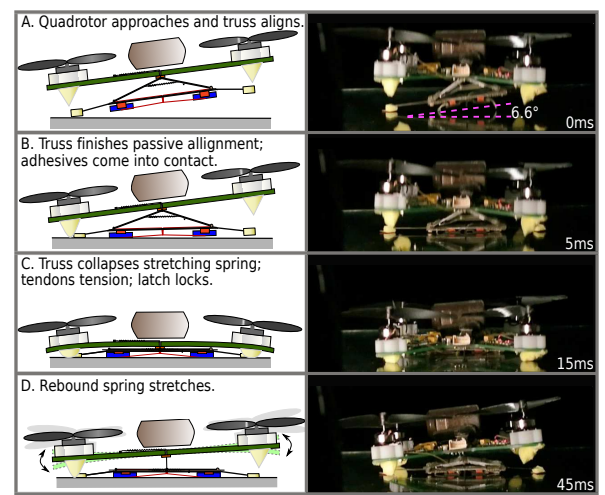


Fig. 2. Landing sequence involving initial alignment and compression of a damped truss mechanism that absorbs kinetic energy and loads adhesives for attachment. Initial velocity is 0.75–1.5 m/s.

1. Mechanical Engineering Dept., 2. Applied Physics Dept., Stanford University, Stanford, CA, USA

3. Dept. of Aerospace Engineering, University of Maryland, MD, USA

supported. Relaxing the internal force causes detachment.

The landing dynamics, involving linear and angular motions, and sliding where the outrigger makes contact, are complex. Modeling this hybrid discrete and continuous system in MotionGenesis [7] is an area of ongoing work. However, some insight can be obtained from the simplest case with a purely normal approach velocity. The initial kinetic energy, $1/2mv_0^2$, must be absorbed without exceeding maximum normal and tangential forces, f_n and f_t respectively, at the pads. To slow the UAV rapidly without exceeding these constraints, the mechanism should be a nonlinear damped spring. As shown in figure 4 (right), a nonlinear rebound spring absorbs energy efficiently for the maximum rebound force of 2 N that the adhesives can sustain. In drop tests (without adhesion) this maximum force corresponds to a rebound height of 20 mm, denoted by a corresponding red dashed line in figure 4 (left). Additionally, with a nonlinear main spring, this rebound is obtained with a higher initial drop height (equivalent to a higher contact velocity where $v_0 = \sqrt{2gh}$) than is possible with a linear spring.

The energy needed to load the tendons is considerably lower than $1/2mv_0^2$. To dissipate this energy with damping is also a challenge using lightweight foams; therefore it is captured and stored internally using a ratchet (figure 5). To detach the UAV, the ratchet is released, resulting in a modest jumping force to assist takeoff.

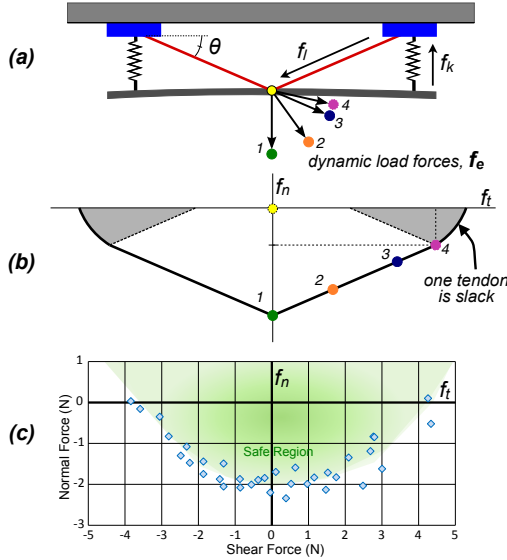


Fig. 3. (a) schematic of two adhesive pads loaded by tendons (f_t) and foam springs (f_k), (b) idealized limit surface showing where various external force vectors, f_e lie, (c) empirical limit surface for two pads loaded with tendons.

The mechanism and the surface properties determine an envelope of initial conditions that can result in attachment. Among these, the velocity normal to the surface and the pitch and roll rates are particularly important. The complementary problem for the UAV controller is to ensure that the vehicle is within this envelope prior to contact, despite disturbances. An area of particular interest is to use optical sensors that take advantage of the wall or ceiling proximity [8].

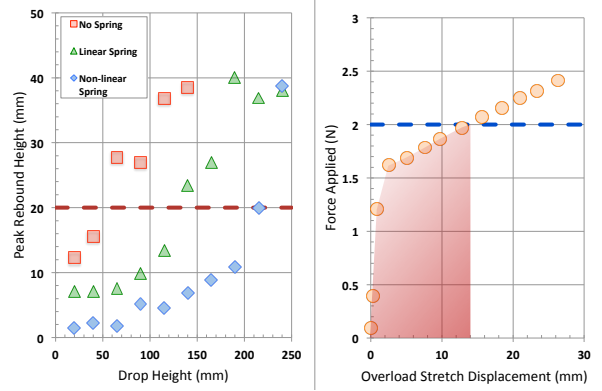


Fig. 4. (right) A nonlinear rebound spring absorbs energy rapidly for a maximum force of 2 N. (left) This force corresponds to a maximum rebound height of 20 mm in drop tests.

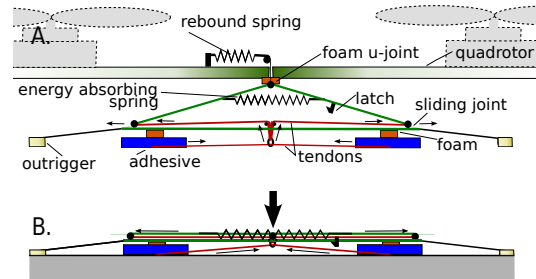


Fig. 5. (A) In unloaded state, outriggers provide initial alignment. As adhesive pads make contact, the mechanism collapses, storing energy in a spring and ultimately loading tendons to create internal force. An additional spring reduces the maximum rebound force. (B) A latch keeps the mechanism locked until ready for takeoff.

II. ACKNOWLEDGMENTS

This work is supported by NSF (IIS 1161679) and ARL MAST (MCE-13-4.4). Hawkes, Eason and Estrada are additionally supported by NSF graduate fellowships.

REFERENCES

- [1] A. Lussier-Desbiens, A. T. Asbeck, and M. R. Cutkosky, "Landing, perching and taking off from vertical surfaces," *IJRR*, vol. 30, no. 3, pp. 355–370, 2011.
- [2] S. Kim, M. Spenko, S. Trujillo, B. Heyneman, D. Santos, and M. Cutkosky, "Smooth Vertical Surface Climbing With Directional Adhesion," *IEEE Trans. on Robotics*, vol. 24, no. 1, pp. 65–74, 2008.
- [3] D. Mellinger, M. Shomin, N. Michael, and V. Kumar, "Cooperative grasping and transport using multiple quadrotors," in *Distributed Autonomous Robotic Syst., ser. STAR*, A. Martinoli, Ed. Springer Berlin Heidelberg, 2013, vol. 83, pp. 545–558.
- [4] M. Kovac, J. M. Germann, C. Hurzeler, R. Siegwart, and D. Floreano, "A perching mechanism for micro aerial vehicles," *Journal of Micro-Nano Mechatronics*, vol. 5, pp. 77–91, 2009.
- [5] L. Daler, A. Klaptoz, A. Briod, M. Sitti, and D. Floreano, "A perching mechanism for flying robots using a fibre-based adhesive," in *IEEE ICRA*, 2013.
- [6] A. Parness, D. Soto, N. Esparza, N. Gravish, M. Wilkinson, K. Autumn, and M. Cutkosky, "A microfabricated wedge-shaped adhesive array displaying gecko-like dynamic adhesion, directionality and long lifetime," *J. Royal Society, Interface*, vol. 6, no. 41, pp. 1223–1232, Mar 2009.
- [7] M. Genesis, "Motion Genesis™," 2010. [Online]. Available: www.motiongenesis.com/
- [8] A. M. Hyslop and J. S. Humbert, "Autonomous Navigation in 3-D Urban Environments Using Wide-Field Integration of Optic Flow," *AIAA Journal of Guidance, Control, and Dynamics*, vol. 33, no. 1, pp. 147–159, 2010.

UAVs Overcoming Physical Limitations: The Tri-TiltRotor in Obstacle Manipulation

Christos Papachristos

Electrical and Computer Engineering Department
University of Patras
Rio 26500, Eratosthenous 6, Greece
Email: papachric@ece.upatras.gr

Anthony Tzes

Electrical and Computer Engineering Department
University of Patras
Rio 26500, Eratosthenous 6, Greece
Email: tzes@ece.upatras.gr

Abstract—The novel concept of UAVs, capable of interfering and actively reconfiguring their environment is the topic of this extended abstract. Realistic cramped-space/indoor areas are characterized by the existence of objects which pose strict limitations to a UAV's navigation path, as in order to overcome these, large forces and moments are required. Typical underactuated UAV platforms are incapable of exerting such forces and moments, as their strict dynamics coupling effectively constrains their flight envelope in order to maintain stability. Via the innovative implementation of reconfigurable, rotor-tilting UAVs, their directly actuated longitudinal dynamics are employed in tackling with such issues: Forward thrust-vectoring can be employed in order to exert large forward-thrusting forces, capable of actively reconfiguring the UAV's environment. At the same time, with proper control synthesis exploiting the additional actuation principle, the UAV can maintain a stable hovering attitude pose.

I. INTRODUCTION

Innovative research tends to surpass the role of UAVs as aerial observation platforms, by performing tasks such as snatch/lift and carry of small objects [2], and inspection/micro-manipulation tasks via contact [1] on objects/surfaces in their environment. The work presented within the context of this extended abstract is aimed at achieving one additional step in this process: To constitute UAVs capable of actively reconfiguring their environment. In order to achieve this, a UAV is required to possess the capability to manipulate realistic-sized objects, such as heavy obstacles blocking the aerial vehicle's desired navigation path within a cramped-spaced environment. This requirement imposes the necessity for large force/moment exertion, which cannot be readily achieved by conventional underactuated UAV platform designs, due to their strong dynamics coupling: In order to produce World-Frame forces, the UAV rigid-body has to be rotated, which poses direct limitations with respect to the aerial vehicle's stability.

In order to tackle this issue, the exploitation of the rotor-tilting capability of reconfigurable UAV designs is employed in an innovative approach: The additional actuation principle over the longitudinal Degree-of-Freedom, gained via rotor-tilting, is utilized in order to produce a significant forward-thrusting force component. At the same time, via a properly synthesized control scheme, appropriate rigid-body moment control for attitude compensation is achieved: Ultimately, the

reconfigurable UAV becomes capable of exerting forward-thrusting forces comparable to its own weight-lifting force, and displacing heavy obstacles weighing more than twice the aerial vehicle itself, while maintaining a stable horizontal hovering attitude pose during the entire operation. Additionally, via differential rotor thrust control, rotating moments can be induced onto the manipulated obstacle, in order to produce more complex displacement-trajectories.

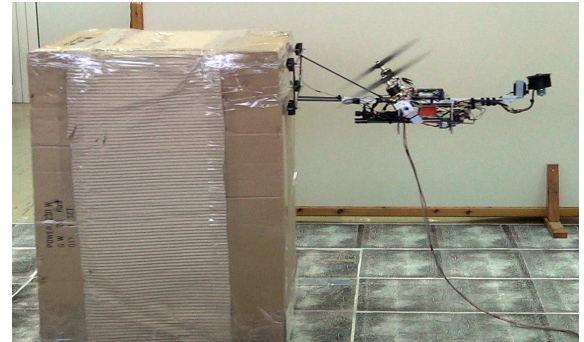


Fig. 1. The UPAT Tri-TiltRotor in Obstacle Forward-Displacement Operation

II. EXPERIMENTAL EVALUATION

For the experimental demonstration of the proposed UAV mobile manipulation application, the UPAT Tri-TiltRotor (UPAT-TTR) [3] platform is employed. In Figure 1, the UPAT-TTR can be observed performing heavy-object manipulation operation via forward-displacement. This visualization intuitively reveals the implemented concept, also presented in Figure 2: The heavy object/obstacle is displaced by exerting a forward-thrusting force, higher than the static friction limit, via the direct longitudinal actuation principle of the rotor-tilting reconfigurable UAV. During the entire operation, moment and vertical forces-compensation via an appropriately designed control synthesis exploiting the utilization of the additional actuation authority, maintains the UAV at a stable hovering attitude pose.

The employed UPAT-TTR platform, illustrated in Figure 3, is an advanced custom-made rotor-tilting UAV design, equipped with high-end technological assets and advanced control capabilities. The Intel Atom-based Single Board Computer Main

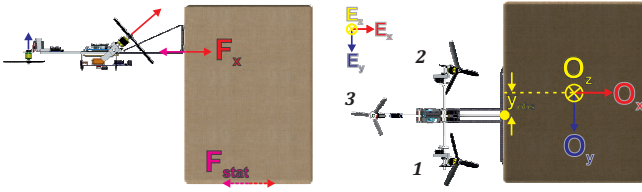


Fig. 2. UPAT-TTR Obstacle-Manipulation Control Principles

Control Unit (MCU), enables the implementation of a Linux Operating System-based software architecture. This achieves: a) seamless integration of Commercial-Off-The-Shelf sensorial equipment, b) powerful software tools such as the MATLAB Real-Time Workshop (RTW) for control design and the Open source Computer Vision (OpenCV) toolbox, as well as c) almost real-time execution control of multiple tasks. With these powerful assets, the full-on-board state estimation is achieved, enabling its operation without external measurement-providing equipment, as well as the implementation of advanced control schemes in the intuitive form of Simulink Block Diagrams.

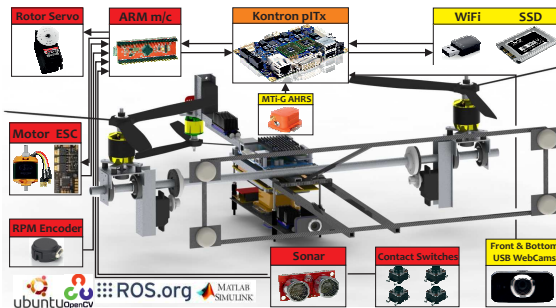


Fig. 3. UPAT-TTR Hardware and Software Setup

The implemented control synthesis consists of cascaded control structures, handling the Attitude dynamics, the Translational dynamics, and the scenario-specific Operation. More particularly for the latter, a High-Level Supervisory Finite State Machine (FSM) controller is implemented, driven by an obstacle detection scheme and providing the appropriate reference signals for the low-level controllers in order to achieve: a) obstacle approaching, b) obstacle docking, c) obstacle manipulation via controlled displacement, and d) obstacle detaching after completion of the manipulation task.

Among various interesting application scenarios, Figure 4 demonstrates a mockup-sequence where the UPAT-TTR's navigation path is blocked by a heavy obstacle. In this sequence, the UAV is incapable of lifting the obstacle as: a) the rotors are not powerful enough to lift both the heavy obstacle ($m_{obs} \approx 5\text{kg}$) and the UAV body ($m_B \approx 2\text{kg}$), and b) it cannot fit in the opening above the obstacle. However, by exerting a forward-thrusting force, it is necessary only to surpass the static friction limit ($F_{stat} \approx 25\text{N}$, as experimentally determined). Additionally, via properly inducing a rotating moment, the UPAT-TTR achieves to manipulate the obstacle position by displacing it aside. As noted, the UAV maintains

hovering attitude regulation during the entire operation, due to the exploitation of the direct longitudinal actuation capability.



Fig. 4. The UPAT-TTR removing an Obstacle hindering its Navigation Path

III. CONCLUSION

The presented concept consists a breakthrough vision for UAVs, as with the incorporation of special-design manipulators as end-effectors, the aerial vehicle can be enabled to perform more complex large force-requiring activities. One such active 1-DoF rotational end-effector is presented in Figure 5, enabling the control of the angle through which the UAV force is applied when docked, yielding more aggressive control over the orientation of the displacement-trajectory. Other active end-effectors may additionally be equipped, allowing the UAV to perform active interaction activities.



Fig. 5. 1-DoF Active End-Effector for Docking-Pushing Angle Variation
REFERENCES

- [1] K. Alexis, C. Huerzeler, and R. Siegwart. Hybrid modeling and control of a coaxial unmanned rotorcraft interacting with its environment through contact. In *2013 International Conference on Robotics and Automation (ICRA)*, pages 5397–5404, Karlsruhe, Germany, May 2013.
- [2] D. Bersak P. Pounds and A. Dollar. Grasping from the air: Hovering capture and load stability. In *2011 International Conference on Robotics and Automation (ICRA)*, 2011.
- [3] C. Papachristos, K. Alexis, and A. Tzes. Model predictive hovering-translation control of an unmanned tri-tiltrotor. In *2013 International Conference on Robotics and Automation (ICRA)*, pages 5404–5412, Karlsruhe, Germany, May 2013.

MODELING AND CONTROL FOR AERIAL MANIPULATION AND ASSEMBLY IN THE ARCAS SYSTEM

A. Ollero, Universidad de Sevilla (aollero@us.es) and Center for Advanced Aerospace Technology
K. Kondak, Institute of Robotics and Mechatronics, DLR (Konstantin.Kondak@dlr.de)

Abstract—The poster presents the results for modeling and control of aerial robots with multi-joint manipulators. The mathematical analysis, as well as the first experiments with helicopters and quadrotors is presented. The presented grasping with a 7 dof arm and structure assembly experiments are considered to be the firsts demonstrations by using helicopters and multi-copters with multi-joint arms.

Aerial manipulation; aerial robots for assembly; modeling and control of aerial robots.

I. INTRODUCTION

The ARCAS project aims at the development and experimental validation of flying robots systems for aerial manipulation including assembly and structure construction. ARCAS is providing scientific foundations for system analysis, control, perception and planning. Further, ARCAS will provide a framework for assembly operations by means of cooperating flying robots where the technologies being developed will be integrated and tested. The project is paving the way for new applications and services in aerial and space robotics. Building of platforms for the evacuation of people in rescue operations, the cooperative inspection and maintenance, the construction of structures in otherwise inaccessible sites as well as servicing on orbit in space applications, are some examples.

The poster presents results for modeling and control of a flying robot with a mounted manipulator in contact with a grasped object by considering the dynamics of whole system composed of a flying platform and a manipulator. Grasping and structure assembly experiments are also presented.

II. MODELLING AND CONTROL OF AERIAL ROBOTS WITH MANIPULATORS

A. Modeling

Two different environments have been used for the modeling and simulation of the aerial robots and the control systems: Modelica and Matlab-Simulink. Particularly, a dynamical model of a whole system composed of a helicopter and a KUKA-DLR Light Weight Robot (LWR) manipulator (see Figure 1) was developed and the first analysis of the whole system was performed. It has been shown that a completely decoupled control of helicopter and manipulator is

problematic if manipulator has enough DoF to move the Tool Center Point (TCP) along x- and y-axis independently. Low frequency diverging oscillations, so-called phase circles, can appear even for systems where TCP movement along one direction is negligible. Therefore, at least a coupling on kinematical level between helicopter and manipulator controllers is needed.



Figure 1. Autonomous helicopter with the LWR III KUKA-DLR arm

Furthermore, quadcopters (see Figure 2) and, in general, multi-copters with multi-joint arms have been modeled and simulated under a Matlab-Simulink environment. It has been shown that, in the manipulation tasks, the dynamic behavior of the vehicle changes due to the modification of the aerial vehicle mass center and mass distribution by grasping and manipulating objects, and by contact forces that may appear when interacting with the environment.



Figure 2. Pelican quadrotor with 3 joint arm

B. Control methods

The analysis of the interaction and coupling between helicopter and manipulator mentioned above resulted in the

development of a controller which uses the 7th degree of freedom of the LWR manipulator to move its center of gravity only in the vertical plane of the helicopter. This controller implements the coupling between manipulator and helicopter control on kinematical level and guarantees that phase cycles, that otherwise are generated in the control loop, do not exist (see [1]).

Furthermore, a control method for rotorcrafts with articulated arms has been developed. The controller is a Variable Parameter Integral Backstepping (VPIB), which is based on a nonlinear backstepping controller with an integral term, plus a feed forward term to compensate arm movements [2]. The controller has been tested in simulation, and experimental tests have been also performed indoor and outdoor with two different aerial platforms and two different arms to check the validity of the modeling and control approach. Figure 3 shows outdoor experiments with the QARM1 aerial robot.

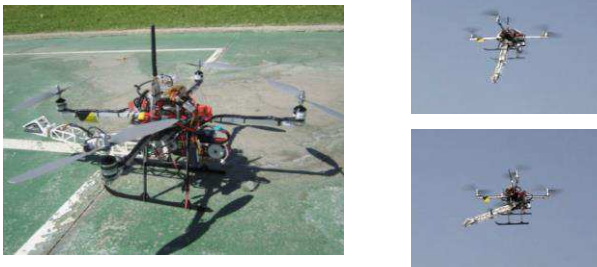


Figure 3. Control experiments with the QARM1 aerial robot.

The comparison of the experimental results of the VPIB controller with and without arm motion compensation and with conventional PID control is shown in Fig 4 pointing out the smaller variations when using the compensation.

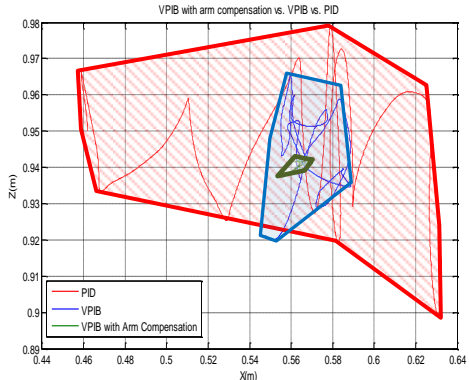


Figure 4. Envelope of the Tool Centre Point positions of the manipulator when using PID control (green), VPIB (blue) and VPIB with arm compensation (green)

III. GRASPING AND STRUCTURE ASSEMBLY

Several additional rotorcraft platforms and arms with 2, 6 and 7 degrees of freedom have been developed and integrated. Furthermore, grasping and structure assembly experiments have been successfully performed.

A. Grasping experiments with the autonomous helicopter with the LWR arm

The above presented control methods have been integrated in an autonomous helicopter with the LWR manipulator. With this system we successfully performed the first autonomous vision guided grasping experiment



Figure 5. Grasping experiment with an autonomous helicopter and the LWR manipulator under visual control.

B. Structure assembly

Autonomous structure assembly has been demonstrated by means of a system with 8 rotors with a robotic arm (see Figure 6). These successful experiments included the grasping of a bar, its transportation and the assembly with one and two connectors simultaneously(see Fig.6).



Figure 6. Fully autonomous structure assembly by means of a platform with 8 rotors and an arm. The photograph shows the system before the assembly of the upper bar with two connectors

CONCLUSIONS

The first results of the ARCAS project have been very promising demonstrating experimentally by the first time fully autonomous grasping and structure assembly with aerial robots with multi-joint arms.

ACKNOWLEDGMENT

This work has been funded by the European Commission under the ARCAS FP7 project, contract 287617

REFERENCES

- [1] K. Kondak, K. Krieger, A. Albu-Schaeffer, M. Schwarzbach, M. Laiacker, I. Maza, A. Rodriguez-Castano, A. Ollero. Closed loop behavior of an autonomous helicopter equipped with a robotic arm for aerial manipulation tasks. International Journal of Advanced Robotic Systems. Vol 10, pp 1-9, 2013.
- [2] J. A.E. Jimenez-Cano, J. Martin, G. Heredia, R. Cano, A. Ollero. Control of an aerial robot with multi-link arm for assembly tasks. To appear in the Proceedings of the 2013 IEEE International Conference on Robotics and Automation. May 2013.

Exploiting image moments for aerial manipulation control

(Extended Abstract)

Rafik Mebarki, Vincenzo Lippiello, and Bruno Siciliano

PRISMA Lab, University of Naples, Italy

Email: rafik.mebarki@unina.it, vincenzo.lippiello@unina.it,
and bruno.siciliano@unina.it

Abstract—We present a new visual servo control scheme that endows flying manipulators with the capability of positioning with respect to visual targets. A camera attached to the UAV provides real-time images of the scene. We consider the approaching part of an aerial assembling task, where the manipulator carries a structure to be plugged into the visual target. In order to augment the system capabilities regarding the 3D interaction with the target, we propose to use image moments. The developed controller generates desired velocities to both the UAV and the manipulator, simultaneously. While taking into account the under-actuation specific to rotary-wing vehicles, it makes use of the system redundancy to realize potential sub-tasks. The joints limits avoidance is also guaranteed. The presented developments are validated by means of computer simulations.

I. INTRODUCTION

The last decade is witnessing an increasing interest in Unmanned Arial Vehicles (UAVs). The present work considers aerial manipulation guided with vision. The robotic system consists of a rotary-wing UAV carrying a robotic arm, which at its turn actuates a structure or an assembly part. The objective consists in automatically positioning the structure on a desired visual target, such that the camera attached to the UAV observes the scene.

We present a new image-based visual servo scheme to achieve the positioning task automatically. It simultaneously controls the UAV and the manipulator at the velocity level, while at the same time it fully exploits the highlighted system's mobility and dexterity.

In the present work, similarly to [4, 3], a new camera configuration class can be defined. In fact, in the field of visual servoing two mains classes are so far considered: *eye-to-hand* and most notoriously *eye-in-hand* configurations. In the former, the camera is observing the robot to control, while in the latter configuration the camera is actuated by the robot. However, in the present configuration the camera is mounted on the UAV, and in fact it observes the manipulator as well. As such, inspired by the above taxonomy of visual servoing schemes, we propose to define this new configuration as “*onboard-eye-to-hand*” to mean that the camera is on-board the UAV (onboard-eye) while observing the robot manipulator (eye-to-hand).

Similarly to our configuration, in [4] a camera is mounted directly on the mobile platform. The grasping task is decomposed into two steps, which involve different visual servoing schemes insuring their accomplishment. In [3], a humanoid robot is controlled for ball catching, where the task is decomposed into different steps with different priorities.

In this paper we present a new visual servo scheme relevant to this new configuration class. In order to improve the system capability of interacting with the target, we adopt image moments [2]. Thanks to their intuitive and geometrical meaning, they can allow for instance performing motion through a line roughly orthogonal to the target during the last approaching phase towards the target (pre-manipulation). This allows avoiding undesirable/unpredictable Cartesian motions that could not be borne in practice, that is a common drawback of many image control schemes. Both the UAV and manipulator are simultaneously controlled at the velocity level. The proposed controller takes advantage of the whole system redundancy, while at the same time it considers the peculiarity of the under-actuation related to rotary-wing UAVs. By including a weighting matrix into the control law, both the mobility of the UAV and the dexterity of the manipulator are exploited. Manipulator joints limits avoidance is guaranteed in addition. Finally, results achieved from computer simulations show the validity of the proposed method.

II. NEW VISUAL ERROR FORMULATION AND KINEMATICS MODELING

The robotic task consists in automatically positioning an assembly part (structure) carried by an aerial robotic system on a visual target, e.g. docking application (see Fig. 1). Both the structure and the target are characterized by a set of m feature points (fiducial), denoted by p_{r_i} and p_{o_i} , respectively, with $i = 1, \dots, m$.

As highlighted earlier, the position of the camera with respect to the robot to control defines a new configuration, while existing visual servoing methods are developed solely for eye-in-hand and eye-to-hand configurations. Works [4, 3], which considers this new configuration, employ subsequent strategies for servoing. In this work we propose a new formulation so both the UAV and the manipulator can be simultaneously

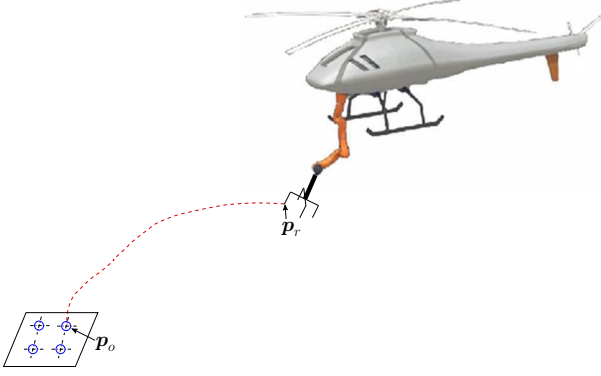


Fig. 1. Helicopter equipped with a robot manipulator holding an assembly part (structure).

controlled to achieve the task. It is characterised by this new visual error definition

$$e_c = s_r - s_o \quad (1)$$

where s_o corresponds to the image features related to the target points, while s_r represents *pseudo* image features of the structure points. Term *pseudo* is employed owing to the fact that s_r might be extracted whether from directly the real-time image or from the manipulator odometry. Although the above definition bears resemblance to classical visual servoing [1], there is in fact an important difference. Indeed, in classical visual servoing only one feature vector intentionally varies to reach a learned and usually constant desired vector. As with the new definition, both the two vectors (s_r and s_o) vary in the image to finally superimpose. Note that there is no need to the pre-phase to learn the desired image, i.e., compute the desired visual features. The robotic system composed of the UAV and manipulator needs to make these vectors converge. We refer to this paradigm to as *Self Visual Servoing* (SVS), to mean that the system *inherently* (self) seeks to superimpose these two vectors.

In order to design the controller, we derive the time variation of the new visual error as a function of the system velocity as follows:

$$\dot{e}_c = J_c \dot{\xi} - \bar{L}_\omega \bar{\omega}, \quad (2)$$

where $\dot{\xi}$ encloses the joint angles velocity of the manipulator and the translational and yaw velocities of the vehicle, while $\bar{\omega}$ corresponds to the roll and pitch angular velocities of the UAV. A kinematic controller can then be designed so desired values of $\dot{\xi}$ would be generated to achieve the task.

III. IMAGE MOMENTS

Low order image moments, as the area, center of gravity, and angle in the image, can provide intuitive and geometrical interpretation of the task. We exploit this fact such that we can specify the 3D interaction of the system with the target. More precisely, we are interested in the pre-grasping and approaching phase before contact. We wish that the assembly structure is being positioned roughly parallel to the target, in order to make the contact homogeneous through the parts and thus compliant.

IV. CONTROL

The principal error to nullify corresponds to image moments according to definition (1). Different subtasks are considered, as described in the following. We employ a control law of the form

$$\dot{\xi}_i := J_{c_i}^+ (-\lambda_i e_{c_i} + \bar{L}_{c\omega_i} \bar{\omega}) + (I_{n+4} - J_{c_i}^+ J_{c_i}) \dot{\xi}_{i+1}, \quad (3)$$

where $\dot{\xi}_i$ represents a desired velocity to achieve current (sub)task, and $J_{c_i}^+$ is a weighted pseudo inverse of the corresponding Jacobian, as described by (2), given by

$$J_{c_i}^+ = W J_{c_i}^\top \left(J_{c_i} W J_{c_i}^\top \right)^{-1}, \quad (4)$$

where W is a weighting diagonal matrix. We express it as a function of the manipulator joint angles and the error in the image. This enables to automatically exploit the mobility of the UAV when far from the target, while on the other hand the manipulator dexterity is exploited when close. In addition, the avoidance of the manipulator joint limits is guaranteed.

Thus, the image-moments error corresponds to e_{c_0} . The second task, e_{c_1} , is the error coordinates between s_r and s_o in order to solve the redundancy related to image moments. Indeed, we noticed that if the final configuration imposes an angle between the structure and the target, the respective image moments vectors might be equal even though they do not define the same image. A third task, e_{c_3} , is to keep the manipulator end-effector aligned with the UAV center of gravity. This to the aim to mitigate the moments a grasped object might apply on the UAV, which thence would be destabilized. Finally, the fourth task consists in keeping the manipulator close to its optimal configuration.

V. CONCLUSION

The developed methods have been implemented in C++ programming language. The obtained results in computer simulation verify their validity.

ACKNOWLEDGMENTS

This work is supported by European ARCAS FP7 project (www.arcas-project.eu).

REFERENCES

- [1] F. Chaumette and S. Hutchinson. Visual servo control, part I: Basic approaches. *IEEE Robotics and Automation Magazine*, 13:82–90, 2006.
- [2] M. K. Hu. Visual pattern recognition by moment invariants. *IRE Transactions on Information Theory*, pages 179–187, February 1962.
- [3] N. Mansard, O. Stasse, F. Chaumette, and K. Yokoi. Visually-guided grasping while walking on a humanoid robot. In *IEEE Int. Conf. on Robotics and Automation*, pages 3041–3047, April 2007.
- [4] Y. Wang, H. Lang, and C. W. de Silva. A hybrid visual servo controller for robust grasping by wheeled mobile robots. *IEEE/ASME Trans. on Mechatronics*, 15:757–769, 2010.

Exploiting image moments for aerial manipulation control

Rafik Mebarki, Vincenzo Lippiello, and Bruno Siciliano

PRISMA Lab, University of Naples, Italy

www.prisma.unina.it

1. Motivation

Unmanned Aerial Vehicles (UAVs) afford numerous advantages: they flight without a pilot onboard; thus might be of amenable size operating in narrow, cumbersome, and especially hazardous environments. This is even particularly true for Vertical Take-off and Landing UAVs since they can hold stationary, and therefore afford operations such as load transports, search and rescue, and freshly aerial manipulation, to name but a few.

2. Aims and objectives

The goal is to endow unmanned aerial robotic systems with the capability of automatically positioning assembly parts on visual targets. A camera attached to the UAV observing the scene provides the principal information to guide the system.

Existing visual servo schemes are devoted to whether eye-in-hand or eye-to-hand configuration. However, the system we consider defines a new configuration, to which existing schemes do not hold.

Achieving the task, automatically, necessitates to develop new visual servo schemes that generates commands to both the UAV and manipulator.

3. Related works

Image-based arm-endowed autonomous robotics control

- W. G. Pence et al., *ICRA*, 2012. Eye-in-hand configuration (classical). Simultaneous control, mobile robotics.
- Y. Wang et al. *IEEE/ASME Trans. on Mechatronics*, 2010. Camera attached to a mobile robot. Different subsequent servoing steps
- N. Mansard et al., *ICRA*, 2007. Camera attached to the head of a humanoid robot. Different subsequent servoing steps with different changing priorities.

4. Contributions

- New definition for a robotics configuration: “*Onboard-eye-to-hand*”
- New visual servoing formalism
- Simultaneous control** of the UAV and manipulator
- Kinematic controller
- Exploiting the mobility of the UAV and the dexterity of the manipulator by inserting a weighted pseudo inverse in the control law
 - Employ the UAV when far from the target
 - Employ instead the manipulator when close the target
- Adopting image moments to enhance the approaching phase (pre-grasping), in order that the actuated structure approaches the target roughly through a perpendicular line.
- Validation through computer simulations



Unnamed helicopter with a robotic manipulator actuating an **assembly part**. The latter needs to be plugged into the **target**.

Visual error formulation:

$$\mathbf{e} = \mathbf{s}_r - \mathbf{s}_o$$

$$\text{Kinematics: } \dot{\mathbf{e}} = \mathbf{J} \dot{\boldsymbol{\xi}} - \bar{\mathbf{L}}_{\omega} \bar{\boldsymbol{\omega}}$$

Enclosing UAV translational and yaw velocities, and manipulator joints rates

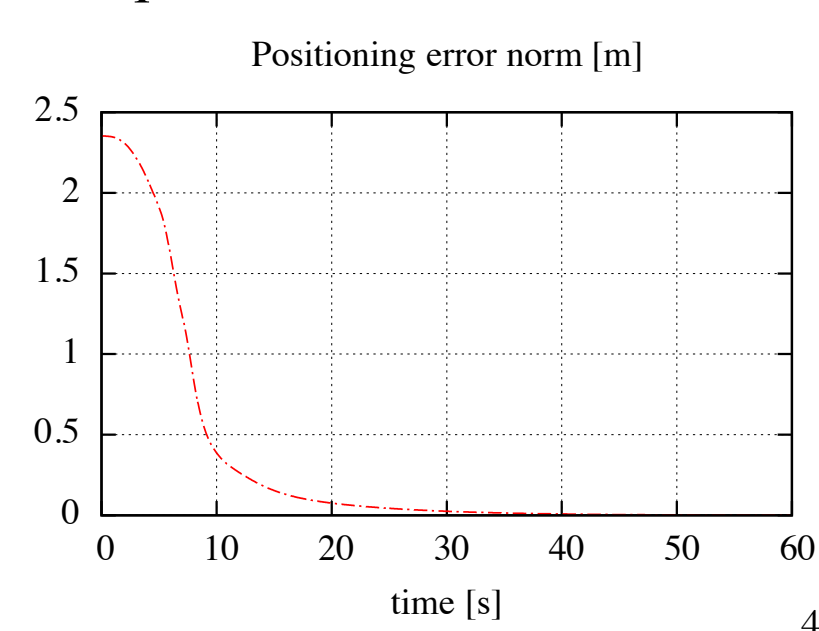
$$\text{Control: } \dot{\boldsymbol{\xi}}_i := \mathbf{J}_{c_i}^+ (-\lambda_i \mathbf{e}_{c_i} + \bar{\mathbf{L}}_{\omega i} \bar{\boldsymbol{\omega}}) + (\mathbf{I}_{n+4} - \mathbf{J}_{c_i}^+ \mathbf{J}_{c_i}) \dot{\boldsymbol{\xi}}_{i+1}$$

$$\mathbf{J}_{c_i}^+ = \mathbf{W} \mathbf{J}_{c_i}^\top \left(\mathbf{J}_{c_i} \mathbf{W} \mathbf{J}_{c_i}^\top \right)^{-1}$$

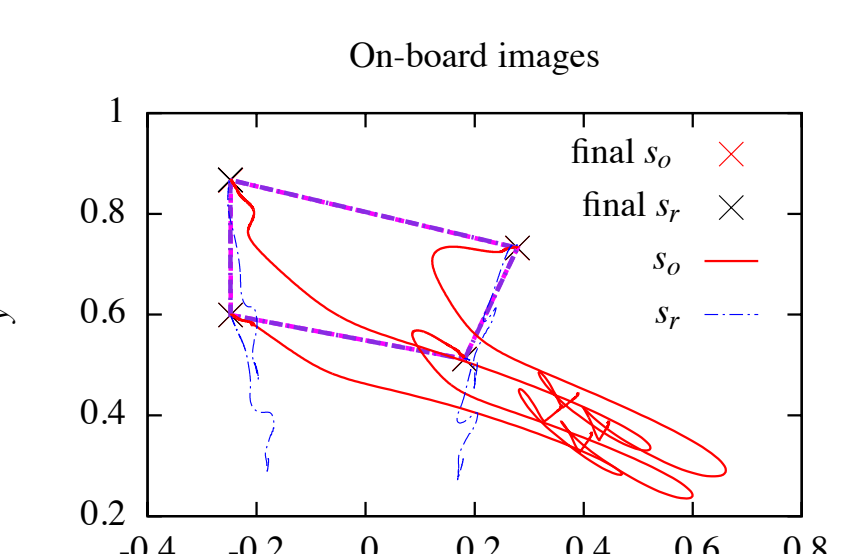
- Main task: nullify image moments error
- Second task: error on (pseudo) image coordinates to solve the ambiguity related to the redundancy of image moments
- Third task: aligning the manipulator end-effector with the UAV center of gravity direction
- Fourth task: keeping the manipulator joints within their optimal configuration

5. Computer simulations

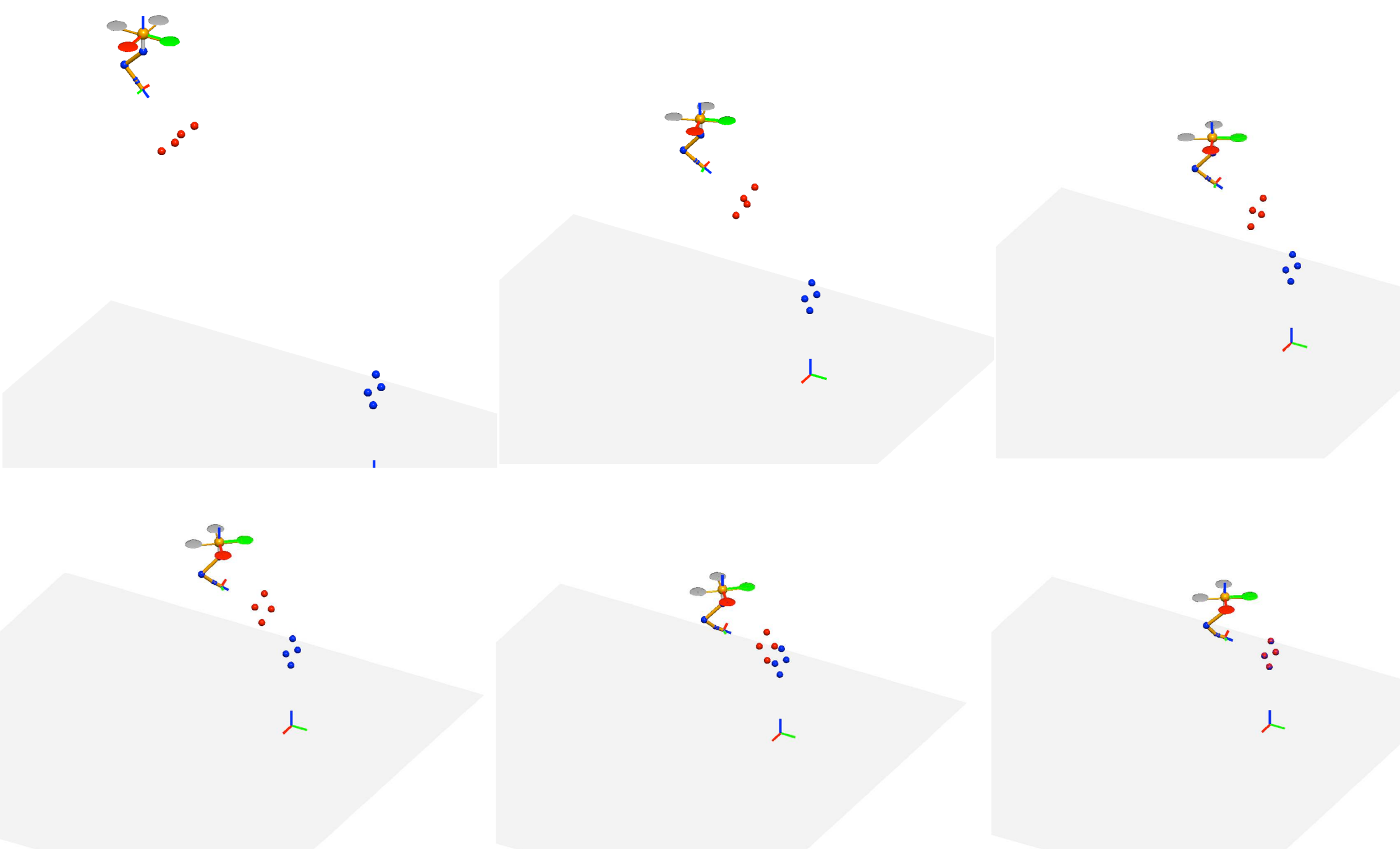
- Implementation in C++ programming language
- The rate of the camera streaming video is 25 Hz
- The UAV and manipulator update at a rate of 1 KHz
- Both the assembly part and the target are characterized by four feature points



$$\text{Am points compared to target points: } \frac{1}{4} \sum_{i=1}^4 |\mathbf{p}_{r_i} - \mathbf{p}_{o_i}|$$



Positions of the feature points in the camera image: evolution of the target points in red, while those of the actuated structure in blue.



3D animation: sequences of the **aerial manipulator** automatically positioning an **assembly part** (characterized by the four red points) on a **visual target** (four blue points).

6. Conclusions and future works

- New visual servo formalism
- Endowing aerial robotics with the capability of automatically positioning carried parts on visual targets
- Validation through computer simulations
- Considering the (interaction) dynamics of both the manipulator and UAV: **preliminary results obtained**
- To perform experimental tests both in indoors and outdoors scenarios
- To address the visibility issue: target hidden by the manipulator and other objects

7. Acknowledgements

This work is supported by ARCAS FP7-European project (www.arcas-project.eu)



Dexterous Hexrotor UAV for Precision Flight

Guangying Jiang, Richard M. Voyles

Abstract—Mobile manipulation is a hot area of study in robotics as it unites the two classes of robots: locomotors and manipulators. An emerging niche in the field of mobile manipulation is aerial mobile manipulation. Although there has been a fair amount of study of free-flying satellites with graspers, the more recent trend has been to outfit UAVs with graspers to assist various manipulation tasks. While this recent work has yielded impressive results, it is hampered by a lack of appropriate testbeds for aerial mobile manipulation. The Collaborative Mechatronics Lab is addressing this instrumentation gap with the development of a dexterous UAV platform to host a low-cost, lightweight Stewart-Gough platform that can be combined as a macro/micro mobile manipulation system. Tantamount to the concept of force closure in a dexterous grasp, the new type of dexterous 6-DoF UAV provides the unique capability of being able to resist any applied wrench, or generalized force-torque which enables complete force closure when coupled to an appropriately dexterous grasper. Typical helicopters or quadrotors cannot instantaneously resist or apply an arbitrary force in the plane perpendicular to the rotor axis, which makes them inadequate for complex mobile manipulation tasks. We have developed a hexrotor UAV that can exert arbitrary wrenches in the 6-DoF force/torque space. We also describe the results of a staged peg-in-hole task that exerts forces without pitching and rolling the UAV, reducing uncertainties.

I. INTRODUCTION

Quadrotors are non-holonomic, which implies, for aerial mobile manipulation, that the quadrotor cannot resist an arbitrary generalized force/torque and cannot support “force closure” for an appropriate grasper. We have developed a Dexterous Hexrotor UAV that can instantaneously resist arbitrary forces or produce arbitrary accelerations – which provides a basis for true force closure through holonomy. To achieve this, the thrusters of our hexrotor are canted so that the combined thrust vectors span the space of Cartesian forces and torques. Not only is this platform more capable of physical interaction, but it is also more precise in the presence of aerodynamic ground effects and disturbances caused by the close interaction with static obstacles.

II. FORCE AND FORM CLOSURE

Force closure is the ability of a mechanism to directly resist any arbitrary wrench. While this strictly applies to the grasper, there is an underlying assumption that the robot to which the grasper is attached is also capable of resisting an arbitrary wrench. Often, the relevance to the locomotor is ignored by the mobile manipulation community because of the large mass and high friction of the mobile base. The relevance to the mobile base cannot be ignored for aerial mobile manipulation or for precision flight at low altitudes as the friction, mass and holonomy of UAVs is insufficient.



Fig. 1. The dexterous hexrotor. Note the rotor axes are not parallel.

III. DESIGN

To create six independent degrees of freedom in force/torque space, one needs six actuators. A conventional hexrotor has six parallel-thrust propellers. Because all thrusters are parallel, no components of the six thrust vectors point along the X or Y axes. We rotate each thruster a cant angle ϕ around its radius to form a nonparallel design so that in-plane components result. This results in holonomy for the UAV and a solid basis for force closure with an appropriate grasper.

The computed total force/torque $[F_{1x} F_{1y} F_{1z} \tau_{1x} \tau_{1y} \tau_{1z}]^T$ applied on the UAV by $Motor_1$ as

$$\begin{bmatrix} F_{1x} \\ F_{1y} \\ F_{1z} \\ \tau_{1x} \\ \tau_{1y} \\ \tau_{1z} \end{bmatrix} = \begin{bmatrix} F_{1fx} \\ F_{1fy} \\ F_{1fz} \\ F_{1\tau x} + \tau_{1\tau x} \\ F_{1\tau y} + \tau_{1\tau y} \\ F_{1\tau z} + \tau_{1\tau z} \end{bmatrix} = PWM_1 * \begin{bmatrix} -K_1 C \theta_1 S \phi \\ K_1 S \theta_1 S \phi \\ K_1 C \phi \\ C \theta_1 (dK_1 C \phi - K_2 S \phi) \\ C \theta_1 (-dK_1 C \phi + K_2 S \phi) \\ dK_1 S \phi + K_2 C \phi \end{bmatrix} \quad (1)$$

which is repeated for all six motors.

IV. OPTIMIZING THE CANT ANGLE, ϕ

The cant angle, ϕ , is the tilt of each thruster with respect to vertical. Dependent on the motors, the desired payload, the manipulator, and diameter of the UAV frame, it is a design variable we must optimize. To do so, we adapt Yoshikawa's concept of "manipulability" by looking at the isotropism of the forces and torques exertable by the Dexterous Hexrotor.

The condition number of the conversion matrix, the ratio of maximum eigenvalue to the minimum eigenvalue, along with the force and torque ellipsoids is shown:

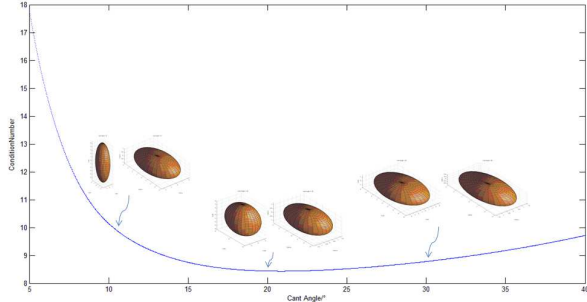


Fig. 2. Condition number with force/torque ellipsoids.

Based on our motors, the load of our manipulator, diameter of the UAV frame, we optimize the cant angle at 20° .

V. AERIAL MANIPULATOR

To complete an aerial mobile manipulation system we have begun development of a lightweight, parallel HexManipulator, as shown in Fig. 3. This 6-DoF end effector will provide a macro/micro combination for enhanced performance. The HexManipulator will provide the fine adjustments at higher bandwidth that the coarse Hexrotor is unable to do.

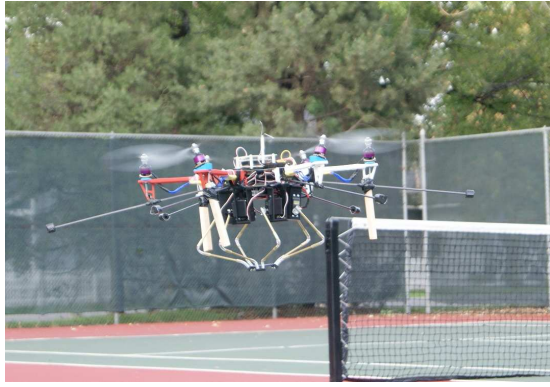


Fig. 3. Hexrotor flying with manipulator.

This HexManipulator is installed underneath the hexrotor platform as shown in Fig 3 for tasks as pick, place, insertion, etc. A base connecting the HexManipulator is bolted under the bottom of hexrotor, which makes it easy to install and replace.

VI. EXPERIMENT

A mock peg-in-hole task is performed to demonstrate performance. Fig. 4 shows the experimental setup. Active control of the HexManipulator was not used in this test as the peg was held rigidly by the hexrotor. With the peg trapped half-way in a hole, we command Dexterous Hexrotor forces and measure the result on the "hole."

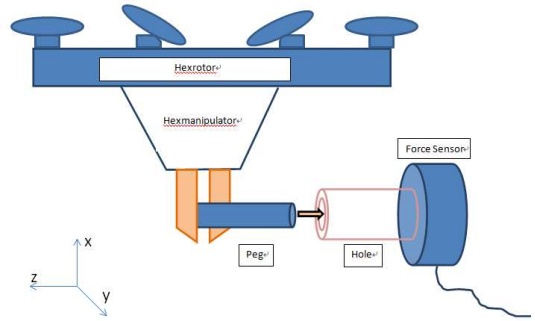


Fig. 4. Peg-in-hole setup, with force sensor's coordinate system indicated.

The Dexterous Hexrotor result includes the force exerted and the attitude of the UAV. Note there is no meaningful pitch of the vehicle. In addition, the rise time is dramatically faster than an equivalent quadrotor.

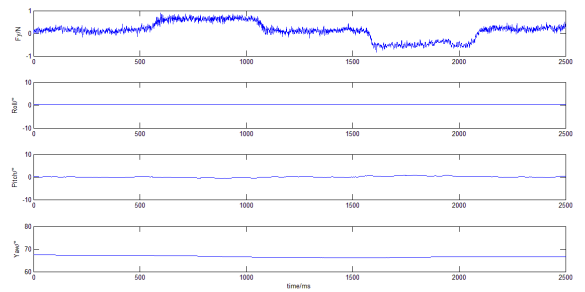


Fig. 5. Hexrotor peg-in-hole measurements of F_y , Roll, Pitch, Yaw.

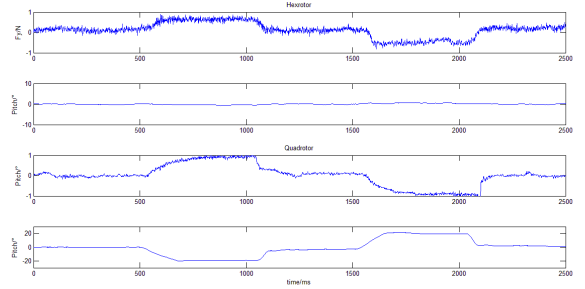


Fig. 6. Hexrotor and quadrotor peg-in-hole measurements of F_y , Pitch.

ACKNOWLEDGMENTS

This work was supported by "NSF Grant CNS-1138674".

Solar Powered Flight for Aerial Robotics: A New Level of Autonomy and Freedom

Scott Morton, and Nikolaos Papanikolopoulos

Center for Distributed Robotics, University of Minnesota
Minneapolis, MN 55455
Email: morto091@umn.edu, npapas@cs.umn.edu

Abstract

A solar powered aerial vehicle would allow for an unprecedented level of autonomy and freedom as a mobile robotics platform. Use of solar power as an energy source would liberate an aerial vehicle from range, flight time and altitude limitations of conventional aircraft. Furthermore, it theoretically allows for indefinite flight. Secondly, an aerial robot that is self-reliant in terms of both its guidance and energy requirements no longer require human interaction to remain in flight. To summarize, a solar powered aerial robot could potentially remain airborne for long durations and operate with complete autonomy. This is an advanced capability for autonomous systems and opens the door to new possibilities in aerial mobile robotics research and applications.

A fixed wing aerial vehicle is an especially attractive mobile robotics platform because of the three dimensional freedom it provides and the high land speeds that can be maintained. Over the past two decades, unmanned aerial vehicles (UAVs) have seen increasing interest from the aerospace and robotics research communities. A subset of this research has focused on the development of solar powered UAVs [1]. Solar powered UAVs have shown significant performance advantages over conventional systems and have set a number of aircraft flight records including greatest altitude reached by a non-rocket engine propelled aircraft [2] and the longest duration flight [3].

However, few of these efforts have focused on small scale solar powered aircraft. The most notable of these [4], achieved a maximum flight time of 27 hours at low altitude. The authors are specifically interested in small scale UAVs (less than 5 meter wingspan) because of the advantages they offer as mobile robotics platform. These include portability, short takeoff, and reduced structural and manufacturing complexity. Therefore, the authors' objective is to combine the flexibility of small scale UAVs with the self-reliance and the endurance, range and altitude provided by a solar power energy source.

The challenge of achieving solar powered flight lies in the ability of the system to capture more solar power than what is consumed for powered flight. For the aircraft to maintain powered flight during periods where this condition is not met, onboard energy storage is required. The amount of energy stored will determine the ability of the aircraft to maintain powered flight when the captured solar power is not enough. Therefore, an appropriate view of solar powered flight should be formed in terms of how well or with what degree of robustness the aircraft can remain in powered flight for a given set of flight conditions. For example, these conditions may include the length of time that the aircraft is able to fly during intermittent overcast or its ability

to maintain position in wind and gust conditions. Therefore, the design goal of a solar powered UAV is to maximize solar powered flight robustness based on specified flight conditions.

Of particular interest to the authors is the capability of achieving continuous flight. Continuous flight has been defined as the ability to maintain powered flight throughout the 24 hour daily cycle [5, 6]. This is only possible if the aircraft is able to capture the energy required for night flight during periods when surplus solar power is available. To achieve continuous flight, the aircraft must be designed with photovoltaic array and battery sizes that maximize the robustness with which indefinite continuous flight is achieved.

In this presentation the authors will overview the state of the art in solar UAV research and present the challenges associated with achieving solar powered flight. A method of quantifying continuous flight robustness will be described and based on this description, criteria to determine the optimal photovoltaic array and battery sizes will be presented.

References

- [1] R. Boucher, "History of Solar Flight," in AIAA/SAE/ASME 20th Joint Propulsion Conference, pp. 1–22, 1984.
- [2] NASA Dryden Factsheet: Helios Prototype. [Online]. Available: <http://www.nasa.gov/centers/dryden/news/FactSheets/FS-068-DFRC.html>
- [3] High Altitude, Long Endurance UAV—Zephyr. [Online]. Available: <http://www.qinetiq.com/news/pressreleases/Pages/three-world-records.aspx>
- [4] A. Noth, "Design of Solar Powered Airplanes for Continuous Flight," Ph. D. Dissertation, ETH Zürich, Zurich, Switzerland, no. 18010. 2008.
- [5] A. Noth, W. Engel, and R. Siegwart. "Design of an ultra-lightweight autonomous solar airplane for continuous flight." Proc. Field and Service Robotics. vol. 28, no. 8, pp. 441-452 2006.
- [6] A. Klesh, and P. Kabamba. "Solar-powered aircraft: Energy-optimal path planning and perpetual endurance." J. Guidance, Control, and Dynamics, vol. 32, no. 4, pp. 1320-1329, 2009.

Hand Driven UAV Formation for Cooperative Grasping and Transportation: the Flying Hand

Guido Gioioso^{*†}, Antonio Franchi[‡], Gionata Salvietti[†], Stefano Scheggi^{*} and Domenico Prattichizzo^{*†}

^{*}Department of Information Engineering and Mathematical Sciences, University of Siena, via Roma 56, 53100 Siena, Italy

Email: {gioioso, scheggi, prattichizzo}@dii.unisi.it

[†]Department of Advanced Robotics, Istituto Italiano di Tecnologia, via Morego, 30, 16163 Genova, Italy

Email: gionata.salvietti@iit.it

[‡]Max Planck Institute for Biological Cybernetics, Spemanstr. 38, 72076, Tübingen, Germany

Email: antonio.franchi@tuebingen.mpg.de

I. INTRODUCTION

Most of the applications recently proposed for the UAVs deal with motion control of teams [1] or with the interaction of a single robot with an object [2]. The possibility of grasping and carrying an object by multiple UAVs has been only recently studied. In [3], a team of quadrotors rigidly attached to an object is used to transport it, while in [4] the payload is connected to the team of robots via cables.

In this extended abstract we summarize the formalization and study of the problem of using N quadrotors in order to cooperatively grasp and manipulate an object using one contact for each quadrotor. We assume that the contact between a robot and the grasped object is established through a tool, rigidly attached to the quadrotor as described in [5]. Each quadrotor can be considered as a single finger of a robotic hand, referred to as *the flying hand*.

The team of quadrotors, differently from [6], is teleoperated by a human. A teleoperation framework for multiple aerial vehicles has been proposed in [7] where UAVs were used as mobile sensors and no contact with the environment was considered. The swarm of quadrotors that we consider physically interact with the object while it is teleoperated by a human hand tracked by a depth camera. The movements of the hand are mapped onto movements of the swarm.

II. TELEOPERATION FRAMEWORK

The proposed teleoperation framework is shown in Fig. 1. We assume that the position and orientation of each quadrotor at the beginning of the grasping action, i.e., the positions of the contact points, is known. Furthermore, we assume that the formation of UAVs always lies on a plane parallel to the ground and that the object allows a planar grasp.

The idea is to relate human hand motions to the reference parameters for the UAVs, represented by the N tool tip positions y_1^d, \dots, y_N^d and the N yaw angles $\psi_1^d, \dots, \psi_N^d$. A Kinect RGB-D camera is employed to capture the human hand motion. The displacement of the centroid of the palm $o_h \in \mathbb{R}^3$ with respect to the starting position and its rotation angle $\omega_h \in \mathbb{R}$ about the camera's z -axis with respect to its initial orientation are computed. Also the open/close movements of the hand are captured evaluating the radius $r_h \in \mathbb{R}$ of the

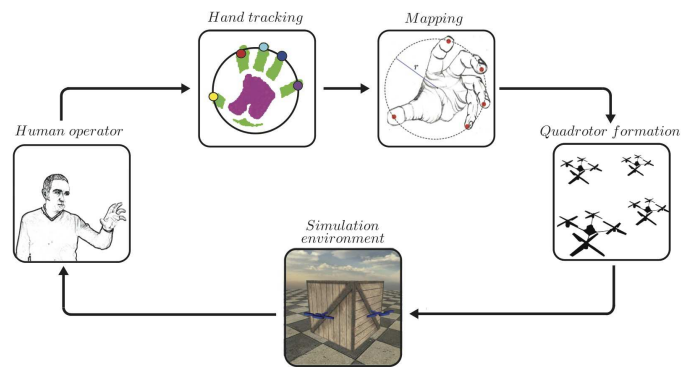


Fig. 1: Schematic representation of the telemanipulation framework.

bounding circle containing the fingertip positions projected on their best-fitting plane.

These parameters are used as input for a mapping algorithm that computes the reference trajectories for the UAVs at a certain time t . The initial configuration of the N contact points $y_{10}^d, \dots, y_{N0}^d$ is instead determined using a grasp planner. The initial yaw angles $\psi_{i0}^d \in \mathbb{R}$ of the UAVs are such that forces in the direction $[\cos \psi_{i0}^d \sin \psi_{i0}^d 0]^T$ are internal, i.e., they do not translate or rotate the object.

Let $y_{c0}^d \in \mathbb{R}^3$ be the center of rotation of the formation in the starting configuration. Let furthermore $\delta_{i0} \in \mathbb{R}^3$ be the distance of the i -th tool tip from the center of rotation. The desired reference parameters $y_i^d(t)$ and $\psi_i^d(t)$ for the quadrotors are then computed with the following rate-control scheme:

$$y_i^d(t) = y_c^d(t) + R_z(\psi_h(t)) \delta_i(t) \quad (1)$$

$$\psi_i^d(t) = \psi_{i0}^d + \dot{\psi}_h(t) \quad (2)$$

where

$$y_c^d(t) = y_{c0}^d + \alpha_o \int_0^t o_h(\tau) d\tau \quad (3)$$

$$\psi_h(t) = \alpha_\omega \int_0^t \omega_h(\tau) d\tau \quad (4)$$

$$\delta_i(t) = \delta_{i0} + \alpha_r r_h(t) \begin{pmatrix} \cos \psi_{i0}^d \\ \sin \psi_{i0}^d \\ 0 \end{pmatrix} \quad (5)$$

and α_o , α_ω and α_r are positive gains. The hand palm displacement affects the position of the rotation center of the team resulting in object movements in \mathbb{R}^3 , the rotation of the hand affects the yaw angle of the formation, keeping the relative orientation of the robots fixed, while the open close movements change the desired positions of the i -th UAV only in the direction $[\cos \psi_i^d(t) \sin \psi_i^d(t) 0]^T$, regulating the internal force amount.

In our proposed method, each quadrotor UAV runs a standard position controller, which is based on a cascaded control design, similarly to what has been used in [7]. This controller results to be robust enough for our application and also easily tunable. A fast PD inner control loop computes the roll and pitch input torques in order to regulate the roll and pitch of the UAV. In absence of any contact with the external environment the desired roll and pitch are achieved thanks to the action of this inner loop. A slower PD outer control loop computes both the thrust and the desired pitch/roll pair in order to achieve an appropriate acceleration for the UAV that would bring the tool tip to its desired position in free space. Finally, the yaw is controlled independently also using a simple PD approach.

Given the PD nature of the position and yaw controllers, the tool-tip behaves approximately as a linear spring/damper system, as long as the discrepancy between the desired quantities and the actual quantities is small enough, and the UAV stays in a near-hovering (quasi static) condition. Because of this behavior, it is enough to select the desired position of the tool tip inside the object surface in order to exert the force that is needed to grasp it. We omit here the details of the controller for the sake of brevity.

In the simulation environment, the amount of exerted force is displayed to the user as a visual feedback by changing the transparency of the grasped object.

III. HUMAN-IN-THE-LOOP SIMULATIONS

In the simulations that we conducted, the motion of the human hand was tracked by a Kinect sensor communicating via UDP/IP with a Matlab/SIMULINK application which implements the hand-to-quadrotors mapping algorithm as well as the physical simulation of the environment and the object to be grasped. The contact has been modeled as a contact point with friction and the friction constraints were modeled according to the Coulomb model. The user was asked to remotely move a wooden cubic box from its starting position to a target location, requiring the object to be lifted during the transport to overcome a wall. In the following some plots regarding a prototypical HIL simulation are presented with the aim of demonstrating the applicability of our framework in a realistic scenario.

Fig. 2 (left) represents the human translational command (top) and the corresponding object linear velocity (bottom). The dashed black lines delimit a dead zone introduced to facilitate the task. First a positive vertical velocity is commanded to lift the object. Then the user commands a horizontal velocity along the x axis to overcame the wall. Finally a negative vertical velocity is commanded. It is easy to see that the object velocity follows the commanded one. In Fig. 2 (right) the

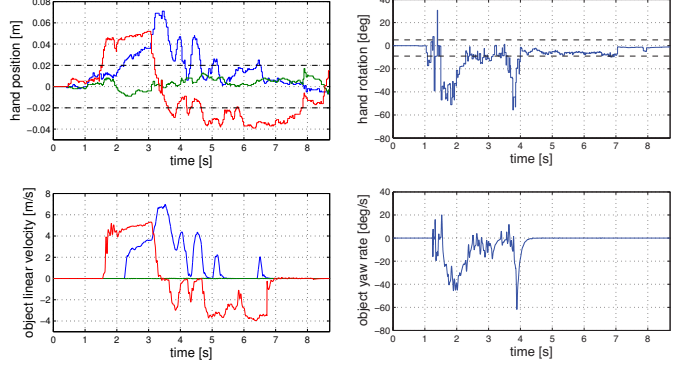


Fig. 2: Top left: displacement vector o_h of the hand centroid with respect to the rest position. Horizontal dashed black indicate the dead zone. Bottom left: linear velocity of the teleoperated box. The following color convention was used: blue $\rightarrow x$, green $\rightarrow y$, red $\rightarrow z$. Top right: rotation angle ω_h of the fingers with respect to the rest position. Horizontal dashed black indicate the dead zone. Bottom right: yaw rate of the teleoperated box.

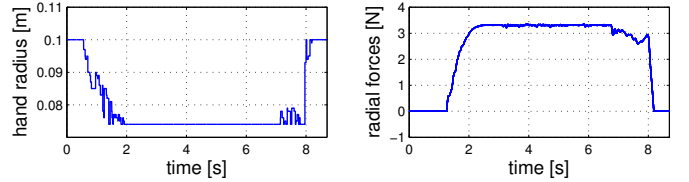


Fig. 3: Hand radius (left) and internal forces exerted by the quadrotors on the object (right).

rotation rate commanded by the user (top) and the yaw rate of the object (bottom) manipulated by the swarm of UAVs are represented. Finally, in Fig. 3 the commanded radius (left) and the corresponding internal forces exerted by the UAVs onto the object (right) are plotted.

The reader is encouraged to watch the video clip related to this abstract.

REFERENCES

- [1] N. Michael, D. Mellinger, Q. Lindsey, and V. Kumar. The GRASP multiple micro-UAV testbed. *IEEE Robotics & Automation Magazine*, 17(3):56–65, 2010.
- [2] Christopher M Korpela, Todd W Danko, and Paul Y Oh. Mm-uav: Mobile manipulating unmanned aerial vehicle. *Journal of Intelligent & Robotic Systems*, pages 1–9, 2012.
- [3] Daniel Mellinger, Michael Shomin, Nathan Michael, and Vijay Kumar. Cooperative grasping and transport using multiple quadrotors. *Distributed Autonomous Robotic Systems*, 2010.
- [4] Nathan Michael, Jonathan Fink, and Vijay Kumar. Cooperative manipulation and transportation with aerial robots. *Autonomous Robots*, 30(1):73–86, 2011.
- [5] D. J. Lee and C. Ha. Mechanics and control of quadrotors for tool operation. In *2012 ASME Dynamic Systems and Control Conference*, Fort Lauderdale, FL, Oct. 2012.
- [6] Vicente Parra-Vega, Anand Sanchez, Carlos Izaguirre, Octavio Garcia, and Francisco Ruiz-Sanchez. Toward aerial grasping and manipulation with multiple uavs. *Journal of Intelligent & Robotic Systems*, pages 1–19, 2012.
- [7] A. Franchi, C. Secchi, H. I. Son, H. H. Bülfhoff, and P. Robuffo Giordano. Bilateral teleoperation of groups of mobile robots with time-varying topology. *IEEE Trans. on Robotics*, 28(5):1019–1033, 2012.

Trajectory Control of a Class of Articulated Aerial Robots

Marin Kobilarov, Johns Hopkins University

I. INTRODUCTION

This work, with full details given in [1], studies trajectory control of aerial vehicles equipped with robotic manipulators. The proposed approach employs free-flying multi-body dynamics modeling and backstepping control to develop stabilizing control laws for a general class of underactuated aerial systems. A simulated hexrotor vehicle with a simple manipulator is employed to demonstrate the proposed techniques. The specific contributions of this work are to: 1) provide a general multi-body aerial vehicle modeling framework, 2) specify a choice of pose representation that enable tracking control with provable stability, 3) employ a coordinate-free formulation which avoids singularities, 4) give guidelines for implementing tasks that require simultaneous tracking of the system center-of-mass and the manipulator tip position. The proposed method currently does not account for uncertainty and control input bounds saturation which are critical for applications on real vehicles.

II. SYSTEM DYNAMICS

The aerial vehicle is modeled as a mechanical system consisting of $n+1$ interconnected rigid bodies arranged in a tree structure. The configuration of body # i is denoted by $g_i \in SE(3)$, where

$$g_i = \begin{pmatrix} R_i & \mathbf{x}_i \\ 0 & 1 \end{pmatrix}, g_i^{-1} = \begin{pmatrix} R_i^T & -R_i^T \mathbf{x}_i \\ 0 & 1 \end{pmatrix}.$$

where $\mathbf{x}_i \in \mathbb{R}^3$ denotes the position of its center of mass and $R_i \in SO(3)$ denotes its orientation. Its body-fixed angular and linear velocities are denoted by $\omega_i \in \mathbb{R}^3$ and $v_i \in \mathbb{R}^3$. The pose inertia tensor of each body is denoted by the diagonal matrix \mathbb{I}_i defined by

$$\mathbb{I}_i = \begin{pmatrix} \mathbb{J}_i & 0 \\ 0 & m_i \mathbf{I}_3 \end{pmatrix}$$

where \mathbb{J}_i is the rotational inertia tensor, m_i is the mass of body # i , and \mathbf{I}_3 denotes the 3x3 identity matrix. Each body is subject to potential energy, e.g. due to gravity, defined by the function $V:SE(3) \rightarrow \mathbb{R}$. Assume that the base body #0 is subject to forces from propellers that result in body-fixed torque $\tau \in \mathbb{R}^3$ and lift force $u > 0$ aligned with the constant body-fixed vertical axis $e = (0, 0, 1) \in \mathbb{R}^3$.

The system has n joints described by parameters $r \in M$, where $M \subset \mathbb{R}^n$ is the *shape space*. The relative transformation between the base body #0 and body # i is denoted by $g_{0i}:M \rightarrow SE(3)$, i.e.

$$g_i = g_0 g_{0i}(r).$$

We assume that all joints are controlled using torque inputs denoted by $\tau_r \in \mathbb{R}^m$.

The equations of motion are obtained using position corresponding to the instantaneous center of mass of the whole system. Such a choice diagonalizes the mass matrix with respect

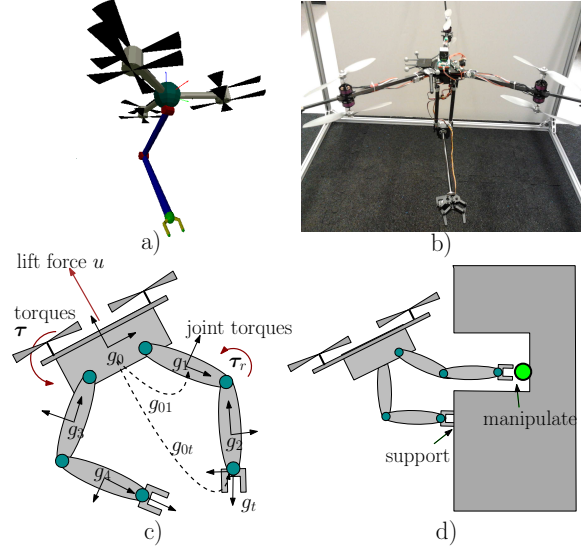


Fig. 1. a) simulated model of hex-rotor vehicle, b) a prototype robot with 3-dof manipulator in development, c) diagram of a typical multi-body aerial system, d) an imaginary scenario where aerial agility could play a key role.

to the position. Thus, the rotation angle around the lift direction e and the transformed position coordinates become differentially flat outputs of the articulated multi-body system.

Let the matrices $\mathbb{J}, C, M_{\omega\dot{r}}, M_{v\dot{r}}, M_{\dot{r}\dot{r}}$ be defined by partitioning the mass matrix according to

$$M_0(r) = \left[\begin{array}{cc|c} \mathbb{J} & C^T & M_{\omega\dot{r}} \\ C & m\mathbf{I}_3 & M_{v\dot{r}} \\ \hline M_{\omega\dot{r}}^T & M_{v\dot{r}}^T & M_{\dot{r}\dot{r}} \end{array} \right], \quad (1)$$

where the total mass m is defined by $m = \sum_{i=0}^n m_i$. Our goal is to isolate the position dynamics which can be accomplished through diagonalization with respect to the v_0 -coordinates. This is equivalent to choosing new velocities $\xi = (\omega, v, r)$ where

Proposition 1. *The equations of motion in coordinates (q, ξ) take the form:*

$$\dot{R} = R\omega, \quad (2)$$

$$m\ddot{x} = ma_g + Reu, \quad (3)$$

$$\begin{bmatrix} \omega \\ \dot{r} \end{bmatrix} = \bar{M}(r)^{-1} \begin{bmatrix} \mu \\ \nu \end{bmatrix}, \quad (4)$$

$$\begin{bmatrix} \dot{\mu} \\ \dot{\nu} \end{bmatrix} = \begin{bmatrix} \mu \times \omega \\ \frac{1}{2} \xi^T \partial \bar{M}(r) \bar{\xi} \end{bmatrix} + \begin{bmatrix} \tau - C^T e u / m \\ \tau_r - M_{v\dot{r}}^T e u / m \end{bmatrix}, \quad (5)$$

where $\bar{\xi} = (\omega, \dot{r})$ and the mass matrix $\bar{M}(r)$ is

$$\bar{M} = \begin{bmatrix} \mathbb{J} - C^T C / m & M_{\omega\dot{r}} - C^T M_{v\dot{r}} / m \\ M_{\omega\dot{r}}^T - M_{v\dot{r}}^T C / m & M_{\dot{r}\dot{r}} - M_{v\dot{r}}^T M_{v\dot{r}} / m \end{bmatrix}. \quad (6)$$

III. TRAJECTORY TRACKING

The tracking problem can be specified in a number of ways depending on the given task and available degrees of freedom. The manipulator end effector(s) frame is given by $g_t \in \text{SE}(3)$ defined by $g_t = g_0 g_{0t}(\mathbf{r})$ where $g_{0t}: M \rightarrow \text{SE}(3)$ is the local workspace transformation. The desired rotation R_d is chosen to satisfy

$$R_d \mathbf{e} = \boldsymbol{\alpha} / u_d, \quad u_d = \|\boldsymbol{\alpha}\|, \quad (7)$$

where

$$\boldsymbol{\alpha} = m \ddot{\mathbf{x}}_d - k_x (\mathbf{x} - \mathbf{x}_d) - k_v (\dot{\mathbf{x}} - \dot{\mathbf{x}}_d) - m \mathbf{a}_g.$$

This condition leaves one additional degree of freedom in R_d that can be specified by the user. Note that there could be multiple manipulators tracking their respective desired tip positions.

A. General Rotation Error

Errors in rotation are encoded using a *retraction map* $\vartheta: \mathbb{R}^3 \rightarrow \text{SO}(3)$, i.e. a smooth map around the origin such that $\vartheta(\mathbf{0}) = I$, where I is the identity. In the following definitions the “hat” notation $\hat{\cdot}: \mathbb{R}^3 \rightarrow \mathfrak{so}(3)$ defined by

$$\hat{\omega} = \begin{bmatrix} 0 & -w^3 & w^3 \\ w^3 & 0 & -w^1 \\ -w^2 & w^1 & 0 \end{bmatrix}, \quad (8)$$

and its inverse $\check{\cdot}: \mathfrak{so}(3) \rightarrow \mathbb{R}^3$ are employed.

Definition III.1. The map $B_\vartheta: \text{SO}(3) \rightarrow L(\mathbb{R}^3, \mathbb{R}^3)$ is such that, for a given $R \in \text{SO}(3)$, the following holds

$$R = I + \hat{\rho} B_\vartheta(R^T),$$

where $\rho = \vartheta^{-1}(R) \in \mathbb{R}^3$. In our implementation we use the Cayley map $\vartheta = \text{cay}$ and its inverse $\vartheta^{-1} = \text{cay}^{-1}$ defined by:

$$\text{cay}(\rho) = \mathbf{I}_3 + \frac{4}{4 + \|\rho\|^2} \left(\hat{\rho} + \frac{\hat{\rho}^2}{2} \right). \quad (9)$$

$$\text{cay}^{-1}(R) = -2 \left[(\mathbf{I}_3 + R)^{-1} (\mathbf{I}_3 - R) \right] \check{\rho} \quad (10)$$

$$B_{\text{cay}}(R) = \frac{4}{4 + \|\rho\|^2} \left(\mathbf{I}_3 - \frac{\hat{\rho}}{2} \right). \quad (11)$$

B. Tracking errors

The control law is based on the error terms

$$\begin{aligned} \mathbf{e}_x &= \mathbf{x} - \mathbf{x}_d, & \mathbf{e}_u &= \mathbf{u} - \mathbf{u}_d, \\ \mathbf{e}_\omega &= \boldsymbol{\omega} - R^T R_d \boldsymbol{\omega}_d, & \mathbf{e}_R &= \vartheta^{-1}(R_d^T R). \end{aligned}$$

Additionally, define the modified terms $\tilde{e}_u \in \mathbb{R}$, $\tilde{e}_\omega \in \mathbb{R}^3$ by

$$\tilde{e}_u = \dot{e}_u + \frac{1}{k_u} \mathbf{e}^T R^T \dot{\mathbf{e}}_x, \quad (12)$$

$$\tilde{e}_\omega = \mathbf{e}_\omega + \frac{1}{k_R} (B_\vartheta(R_d^T R) \mathbf{e} u_d) \times R^T \dot{\mathbf{e}}_x. \quad (13)$$

These terms are key in obtaining a stable controller despite the non-trivial system underactuation.

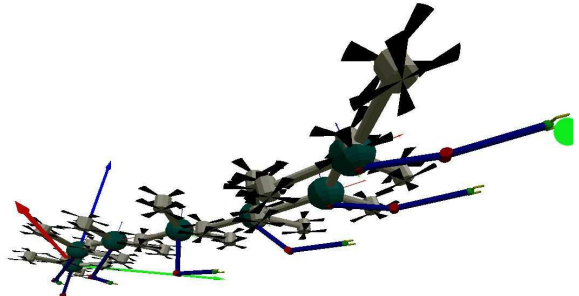


Fig. 2. Several frames along the simulated hexrotor trajectory reaching a desired point in workspace.

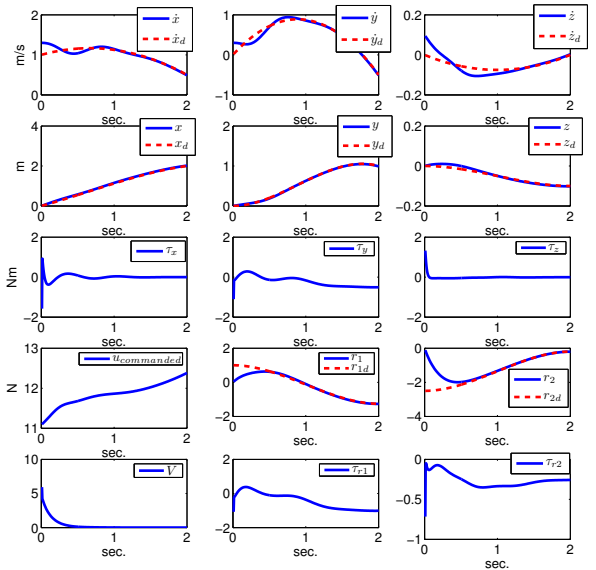


Fig. 3. States, controls, and Lyapunov function V of the scenario in Fig. 2

C. Control Law

Proposition 2. [1] The control inputs (u, τ, τ_r) given by

$$\ddot{u} = -k_u e_u - k_u \tilde{e}_u + \ddot{u}_d - \frac{1}{k_u} (\dot{\mathbf{e}}_x^T R e + \dot{\mathbf{e}}_x^T R (\boldsymbol{\omega} \times \mathbf{e})),$$

$$\begin{bmatrix} \tau \\ \tau_r \end{bmatrix} = \begin{bmatrix} -k_R R^T R_d e_R - k_\omega \tilde{e}_\omega - \boldsymbol{\mu} \times \boldsymbol{\omega} + C^T e u / m \\ -k_r \mathbf{e}_r - k_{\dot{r}} \dot{\mathbf{e}}_r - \frac{1}{2} \tilde{\boldsymbol{\xi}}^T \partial \bar{M}(\mathbf{r}) \tilde{\boldsymbol{\xi}} + M_{vr}^T e u / m \\ + \dot{\mathbf{b}} + \frac{1}{2} \dot{\bar{M}}(\mathbf{r}) \begin{bmatrix} \tilde{e}_\omega \\ \dot{\mathbf{e}}_r \end{bmatrix}, \end{bmatrix}$$

$$\text{where } \mathbf{b} = \bar{M}(\mathbf{r}) \begin{bmatrix} R^T R_d (\boldsymbol{\omega}_d - \frac{1}{k_R} B_\vartheta(R_d^T R) \mathbf{e} u_d \times R^T \dot{\mathbf{e}}_x) \\ \dot{\mathbf{r}}_d \end{bmatrix} \quad (14)$$

asymptotically track a given desired trajectory $(\mathbf{x}_d(t), R_d(t), \mathbf{r}_d(t))$.

IV. APPLICATION: HEXROTOR WITH A SIMPLE MANIPULATOR

Figures 2 and 3 show the simulated controller behavior during an aggressive reaching maneuver of the hexrotor shown in Figure 1. The vehicle is required to track a path of center of mass position and manipulator tip position which extends outside of the vehicle propeller range in order to reach a desired final point.

REFERENCES

- [1] M. Kobilarov, “Trajectory control of a class of articulated aerial robots,” in *International Conference on Unmanned Aircraft Systems*, 2013.

Aerial 6-dimensional quasi-static manipulation on the *FlyCrane* towed-cable system

Montserrat Manubens
IRI, CSIC-UPC
Barcelona, Spain
Email: mmanuben@iri.upc.edu

Didier Devaurs
LAAS, CNRS
Toulouse, France
Email: ddevaurs@laas.fr

Juan Cortés
LAAS, CNRS
Toulouse, France
Email: jcortes@laas.fr

Lluís Ros
IRI, CSIC-UPC
Barcelona, Spain
Email: lros@iri.upc.edu

Abstract—We propose a new approach for the reliable 6-dimensional quasi-static manipulation of an aerial towed-cable system. The novelty of this approach lies in the combination of results deriving from the static analysis of cable-driven manipulators with the application of a cost-based motion-planning algorithm to solve manipulation queries. Using this approach, we can ensure that the produced paths are feasible and do not approach dangerous configurations that could provoke the malfunction of the system. The approach has been simulated on the *FlyCrane*, consisting of a platform attached to three flying robots using six fixed-length cables. The obtained results show the success and the suitability of the approach.

I. INTRODUCTION

Most of the applications where aerial towed-cable systems have been applied use them as crane devices, only monitoring the position of the carried load [1, 8]. Instead, little work has been done on trying to govern the load in both position and orientation on the mentioned systems. Up to our knowledge, the only existing approach able to perform such 6-dimensional manipulation queries is given in [4]. It requires a given discrete set of intermediate load poses for which the IKP and the static equilibrium are solved. However, requiring a given set of load poses may be too restrictive, especially in constrained workspaces, because it can prevent the system from obtaining feasible motions, while there may exist solutions for different intermediate load poses.

In contrast, we provide an approach for 6-dimensional quasi-static manipulation with an aerial towed-cable system that only requires a start and a goal configurations and provides a feasible path to achieve the desired manipulation task. The novelty of the proposed approach lies in the combination of static properties derived from cable-driven manipulators with a cost-based motion-planning algorithm that will ensure the reliability of the computed manipulation paths.

II. OVERVIEW OF THE APPROACH

We will assume an aerial towed-cable system consisting of a platform attached to three flying robots by means of six cables linked by pairs to each robot as in Fig. 1. This structure will be called the *FlyCrane* system. It is worth noting that three is the minimal number of flying robots required to properly operate the six degrees of freedom of the platform.

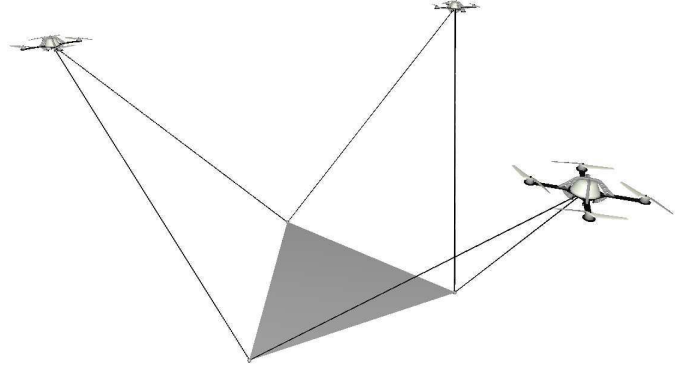


Fig. 1. A *FlyCrane* system in its octahedral version.

Due to their similarities, a towed-cable system can be analyzed as a cable-driven manipulator. Actually, while cable-driven manipulators have to adjust the lengths of their cables to reach a precise pose of the platform, towed-cable systems have fixed-length cables and are actuated by displacing their anchor points. In general, actuating six degrees of freedom requires a minimum of seven cables, unless some convenient forces reduce this number. In our case, gravity acts as an implicit cable, and thus six cables will suffice for the 6-dimensional manipulation of the load.

However, the six degrees of freedom of the load cannot be governed in the whole configuration space. The pose of the load is locally determined only when all cables are in tension. Therefore, it is important to prevent the cables from being slack or too tight. Besides, it must be ensured that the flying robots can counteract the forces exerted on them. So, two types of constraints must be fulfilled along a quasi-static manipulation path:

- *Wrench-feasibility* constraints: guaranteeing that the system is able to statically counteract a set of wrenches applied on the platform while ensuring that the cable tensions always lie within a pre-defined, positive acceptance range. These constraints are derived from the static analysis of cable-driven manipulators [3, 2].
- *Thrust* constraints: guaranteeing that the thrust of the flying robots can equilibrate the forces applied on them, namely gravity and the forces exerted by the cables.

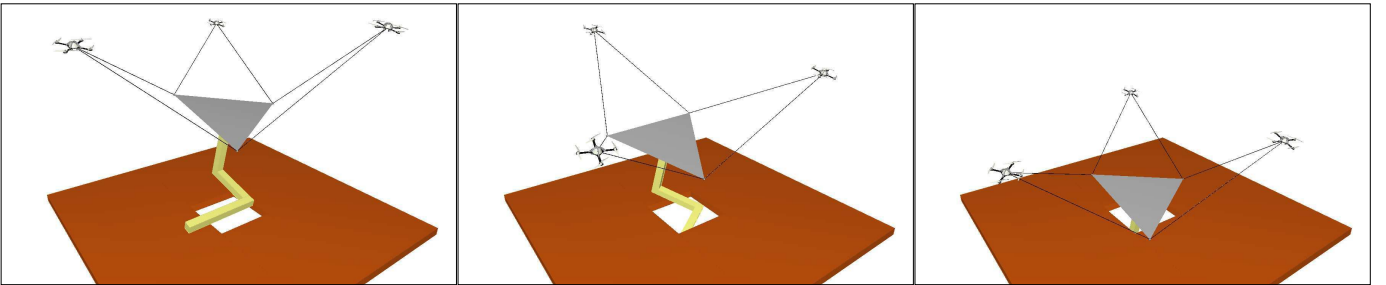


Fig. 2. The *Puzzle* problem: the *FlyCrane* has to get a 3D puzzle piece through a hole.

In general, for a given manipulation query, there may exist a high number of solution paths that satisfy both constraints. In order to privilege the most appropriate ones, we introduce a quality measure on the configuration space, which indicates how far from not satisfying the aforementioned constraints is a configuration. This will define a cost function over the configuration space of the system.

To perform the 6-dimensional quasi-static manipulation of a load, we have to use a motion-planning method. Any general path planner, such as the Rapidly-exploring Random Tree (RRT) algorithm [6], is able to compute collision-free paths satisfying the previous feasibility constraints. But it may not produce good-quality paths. Instead, we can take advantage of the previously defined cost function and use a cost-based path planner, such as the Transition-based RRT (T-RRT) [5], in order to obtain *good-quality* paths. Although T-RRT has been successfully applied to various types of problems in robotics [5], to the best of our knowledge this is the first time it is applied to aerial manipulation problems.

III. RESULTS

We have evaluated the approach on some 6-dimensional quasi-static manipulation problems, and we have compared the obtained paths to those produced by RRT, which does not take the cost function into account, on the same manipulation queries. Figure 2 shows three screenshots illustrating the resolution of the *Puzzle* problem.

The results of the evaluation show that, rather than simply computing collision-free manipulation paths, the approach produces reliable 6-dimensional quasi-static manipulation paths. While RRT may produce paths that occasionally reach dangerous situations, our approach favors paths whose configurations are far from violating the given constraints, thus resulting in safer paths.

More details on the proposed approach can be found in [7].

ACKNOWLEDGMENTS

This work has been partially supported by the European Community under contract ICT 287617 "ARCAS", by the Spanish Ministry of Economy and Competitiveness under contract DPI2010-18449, and by a *Juan de la Cierva* contract supporting the first author.

REFERENCES

- [1] M. Bernard, K. Kondak, I. Maza, and A. Ollero. Autonomous transportation and deployment with aerial robots for search and rescue missions. *Journal of Field Robotics*, 28(6):914–931, 2011.
- [2] O. Bohigas, M. Manubens, and L. Ros. Navigating the wrench-feasible C-space of cable-driven hexapods. In *Cable-driven Manipulators*, pages 53–68. Springer, 2012.
- [3] P. Bosscher, A.T. Riechel, and I. Ebert-Uphoff. Wrench-feasible workspace generation for cable-driven robots. *IEEE Transactions on Robotics*, 22(5):890–902, 2006.
- [4] J. Fink, N. Michael, S. Kim, and V. Kumar. Planning and control for cooperative manipulation and transportation with aerial robots. *International Journal of Robotic Research*, 30(3):324–334, 2011.
- [5] L. Jaillet, J. Cortés, and T. Siméon. Sampling-based path planning on configuration-space costmaps. *IEEE Transactions on Robotics*, 26(4):635–646, 2010.
- [6] S. M. LaValle and J. J. Kuffner. Rapidly-exploring random trees: Progress and prospects. In *Algorithmic and Computational Robotics: New Directions*, pages 293–308. A K Peters, 2001.
- [7] M. Manubens, D. Devaurs, J. Cortés, and L. Ros. 6-d manipulation with aerial towed-cable systems. In *Proc. of Robotics: Science and Systems*, 2013. In press.
- [8] P. Williams. Optimal terrain-following for towed-aerial-cable sensors. *Multibody System Dynamics*, 16(4):351–374, 2006.